JGR Planets

RESEARCH ARTICLE
10.1029/2018JE005802

Geological Evidence of Planet-Wide Groundwater System on Mars

Francesco Salese[1,2], Monica Pondrelli[2], Alicia Neeseman[3], Gene Schmidt[2], and Gian Gabriele Ori[2,4]

[1]Faculty of Geosciences, Utrecht University, Utrecht, The Netherlands, [2]International Research School of Planetary Sciences, Università Gabriele D'Annunzio, Pescara, Italy, [3]Institute of Geological Sciences, Planetary Sciences and Remote Sensing Group, Freie Universität Berlin, Berlin, Germany, [4]Ibn Battuta Centre, Université Cadi Ayyad, Marrakesh, Morocco

Key Points:
- Geological evidence supporting Martian planet-wide groundwater upwelling
- Water-saturated zone intercepted by basins reaching more than -4000m below the Mars DATUM
- Putative relations between groundwater-saturated level (groundwater-fed lakes) and the ocean shorelines around -4000m below the DATUM

Supporting Information:
- Supporting Information S1
- Figure S1

Correspondence to:
F. Salese,
f.salese@uu.nl

Citation:
Salese, F., Pondrelli, M., Neeseman, A., Schmidt, G., & Ori, G. G. (2019). Geological evidence of planet-wide groundwater system on Mars. *Journal of Geophysical Research: Planets*, *124*, 374–395. https://doi.org/10.1029/2018JE005802

Received 24 AUG 2018
Accepted 15 JAN 2019
Accepted article online 21 JAN 2019
Published online 13 FEB 2019

Author Contributions:
Conceptualization: Francesco Salese
Investigation: Francesco Salese, Monica Pondrelli, Alicia Neeseman, Gene Schmidt, Gian Gabriele Ori
Methodology: Francesco Salese, Monica Pondrelli, Alicia Neeseman
Resources: Francesco Salese
Supervision: Francesco Salese
Validation: Francesco Salese, Monica Pondrelli, Gian Gabriele Ori
Writing - original draft: Francesco Salese, Monica Pondrelli, Alicia Neeseman, Gene Schmidt
Writing – review & editing: Francesco Salese

Abstract The scale of groundwater upwelling on Mars, as well as its relation to sedimentary systems, remains an ongoing debate. Several deep craters (basins) in the northern equatorial regions show compelling signs that large amounts of water once existed on Mars at a planet-wide scale. The presence of water-formed features, including fluvial Gilbert and sapping deltas fed by sapping valleys, constitute strong evidence of groundwater upwelling resulting in long term standing bodies of water inside the basins. Terrestrial field evidence shows that sapping valleys can occur in basalt bedrock and not only in unconsolidated sediments. A hypothesis that considers the elevation differences between the observed morphologies and the assumed basal groundwater level is presented and described as the "dike-confined water" model, already present on Earth and introduced for the first time in the Martian geological literature. Only the deepest basins considered in this study, those with bases deeper than −4000 m in elevation below the Mars datum, intercepted the water-saturated zone and exhibit evidence of groundwater fluctuations. The discovery of these groundwater discharge sites on a planet-wide scale strongly suggests a link between the putative Martian ocean and various configurations of sedimentary deposits that were formed as a result of groundwater fluctuations during the Hesperian period. This newly recognized evidence of water-formed features significantly increases the chance that biosignatures could be buried in the sediment. These deep basins (groundwater-fed lakes) will be of interest to future exploration missions as they might provide evidence of geological conditions suitable for life.

Plain Language Summary Most previous studies on Mars relevant groundwater have proposed models, but few have looked at the geological evidence of groundwater upwelling in deep closed basins in the northern hemisphere equatorial region. Geological evidence of groundwater upwelling in these deep basins is a key point that will help to validate present-day models and to better constraint them in the future. Observations in the northern hemisphere show evidence of a planet-wide groundwater system on Mars. The elevations of these water-related morphologies in all studied basins lie within the same narrow range of depths below Mars datum and notably coincide with the elevation of some ocean shorelines proposed by previous authors.

1. Introduction

Early in its history Mars was characterized by an active hydrosphere (Baker, 2001; Carr & Head, 2003, 2010; Fairen et al., 2003; Head et al., 1999; Kreslavsky & Head, 2002; Malin & Edgett, 1999; Parker et al., 1993; J. A. P. Rodriguez, Zarroca et al., 2015; J. A. Rodriguez et al., 2016; Tanaka et al., 2005), followed by the retreat of surface water into subsurface aquifers underneath a thick ice-rich permafrost zone (Clifford & Parker, 2001) where it became part of groundwater stores (Andrews-Hanna et al., 2007). Groundwater could have been a major factor in the origin and evolution of water-related sedimentary systems on Mars (Andrews-Hanna et al., 2007, 2010; Goldspiel & Squyres, 2000; Howard, 1986; Malin & Carr, 1999; Siebach et al., 2014; Stack et al., 2014).

Treiman (2008) found evidence of groundwater flow during the Hesperian in Valles Marineris, and Andrews-Hanna et al. (2010) presented a model showing that the playa environment in Meridiani Planum was controlled by a zone of groundwater upwelling on a regional scale, occurring first in the deepest basins. According to their model, regional- to global-scale groundwater flow might explain the

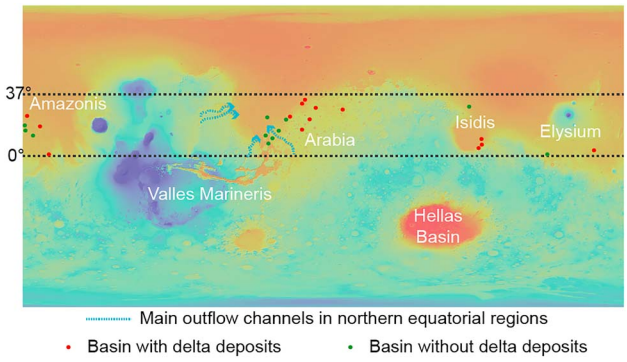

Figure 1. Distribution of the studied basins on Mars based on Mars Orbiter Laser Altimeter topography (blue indicates high elevations). Their distribution follows the dicotomy boundary, and they are clustered in the Arabia and Amazonia quadrangles along two parallel lines aligned NNE-SSW in the first case and NNW-SSE, respectively, with high concentration in Arabia Terra and Amazonia.

formation and location of the light-toned layered deposits (LLDs) in Arabia Terra in a playa depositional setting.

The existence of extensive groundwater aquifers in Arabia Terra (Michalski et al., 2013; Pondrelli et al., 2015; J. A. P. Rodriguez, Zarroca et al., 2015) and Meridiani Planum (Grotzinger et al., 2005; Squyres et al., 2009) is also supported by the presence of spherical hematite inclusions informally called "blueberries," discovered by the Mars Exploration Rover Opportunity in Meridiani Planum (Squyres et al., 2004), as well as the sulfate mineralogy of the cements and the presence of current ripples in the upper Burns formation (Chan et al., 2004; Lamb et al., 2012).

In recent years, several authors (Cabrol & Grin, 1999; De Hon, 1992; Goudge et al., 2015; Scott et al., 1995, 1991) presented catalogues of closed basins across the surface of Mars, but they did not include candidate groundwater-fed closed-basin lakes (Goudge et al., 2015), despite that they represent an important component of the paleolake record on Mars (Michalski et al., 2013; Wray et al., 2011). Furthermore, previous surveys of ancient deep craters have shown no evidence for widespread groundwater upwelling. Based on their analysis, Michalski et al. (2013, 2012) raised several arguments against a global-scale groundwater upwelling scenario because of the lack of extensive groundwater-driven sedimentation (e.g., LLD) inside these deep basins and the deposits' age (Michalski et al., 2013).

In contrast with the interpretation of Andrews-Hanna et al. (2010) regarding regional to global groundwater activity, Michalski et al. (2013) analyzed 95 large basins in the northern hemisphere and inferred that groundwater upwelling on Mars may have occurred sporadically and locally in basins deeper than −4,000 m, such as McLaughlin crater. According to Michalski et al. (2013), this activity would have predated the groundwater upwelling related deposition proposed by Andrews-Hanna et al. (2010) because 80% of the basins that were analyzed in the northern hemisphere impacted Noachian terrain. However, the ages of these 95 craters were not investigated in detail and the study only used the global superordinate stratigraphic units (Noachian, Hesperian, and Amazonian), considering the craters found within these units to be the same age as the units. This is arguably a misconception however, as every geomorphological unit includes craters formed at a later time. This means that the Noachian unit includes numerous craters of Hesperian and Amazonian age as well. Furthermore, the authors did not find all of this geomorphological and sedimentological evidence of groundwater upwelling and standing bodies of water within the studied basins, with the exception being McLaughlin crater.This study aims to present new evidence that explains the nature and origin of the deposits and morphologies inside these deep craters, as well as their spatial distribution, to infer the controls on deposition, and establish their global significance.

In order to understand if groundwater influences are expressed on a local, regional, or global scale, we focus our detailed geological analyses on the structure and stratigraphy of enclosed craters located in the northern equatorial regions, near the dichotomy boundary with floors below −4,000-m elevation.

We have only considered and analyzed enclosed basins that were not fed externally, so as to ensure that all processes within the craters are related to groundwater alone. The studied craters show little or no evidence of aqueous activity in the terrains surrounding their outer rims, so they are not fed by surface drainage. In fact, they lack breached rims, with the exception of short sapping valleys that are a result of retrograding erosion. All the selected basins are located between 0°N and 37°N to limit the effects of current day ice on the observed morphological forms and deposits as the north cap reaches about 37°N at its maximum extent (Michaux & Newburn, 1972; Slipher, 1962). We focused on the northern hemisphere because this is where a large fraction of groundwater upwelling is predicted to have occurred (Andrews-Hanna et al., 2007, 2010; Michalski et al., 2013).

Our work reveals evidence of some previously unrecognized water-formed features that have never been considered holistically, from the scale of the individual basin to the planet-scale context. These features are likely to have resulted from a process of groundwater upwelling followed by water table fluctuations and eventual groundwater recession. The presence of a large number of water-formed features in all these deep basins (Figure 1) is a compelling sign that Mars once had large amounts of water stored as

groundwater that debouched into the intercepting craters to form lacustrine systems (Palucis et al., 2016). The purpose of this work is to identify these water-related features at a basin level, define their depositional environments and then analyze them holistically at a planetary scale to identify whether they are the result of a single planet-wide control (Figure 1).

The geological evidence presented in this work corroborates the Andrews-Hanna et al. (2010) theory of global-scale groundwater upwelling and supports the model presented by Michalski et al. (2013) but contests the assertion that McLaughlin crater is the only basin presenting geological evidence of groundwater upwelling. Although they focused on McLaughlin crater due to the strong spectroscopic evidence for upwelling, the authors also suggest there could be other craters presenting geomorphological evidence of groundwater upwelling that were not investigated in their work Michalski et al. (2013).

If life once existed on Mars, it could have been preferentially confined to some protective water related niches (e.g., Carrozzo et al., 2017; Hamilton et al., 2018). Evidence of the past existence of long-standing bodies of water on Mars, such as lakes or deltas, has significant implications both for climate and life: groundwater-fed lakes could warm Mars' climate (Tosca et al., 2018) and increase the chance that life forms might have existed and presently remain buried in the sediment. These deep basins (due to a lower gravity that implies less compaction of the pore space and lower heat flow that reduces the temperature constraints, see Michalski et al., 2013) arguably offer the best chance of finding evidence of past prebiotic chemistry or even past microbial life on the Red Planet.

2. Methodology

Basins are repositories of sediments that store information and aid interpretations of the geological history because they provide us with a window into the past. We focused on the identification and analysis of water-related features in selected deep closed basins and then extended the analysis to a regional level to arrive at a holistic interpretation of the groundwater processes that could have taken place on Mars.

We investigated the geology of deep impact craters in the northern hemisphere of Mars, between 0°N and 37°N, using imaging data from High Resolution Imaging Science Experiment (HiRISE; McEwen et al., 2007), Context Camera (CTX; Malin et al., 2007), High Resolution Stereo Camera (HRSC; Jaumann et al., 2007; Neukum & Jaumann, 2004), and the digital terrain model from HRSC and Mars Orbiter Laser Altimeter (MOLA; D. E. Smith et al., 1999) data. The sparse distribution of hyperspectral observations, such as those made by the Compact Reconnaissance Imaging Spectrometer for Mars (Murchie et al., 2007), does not allow the systematic use of mineralogy as a tool to interpret the depositional processes/environments. Still, where published data were available, they have been considered to strengthen the genetic inferences. Deep craters (typically diameters of 28 to 114 km; depths of 1.4 to 3.1 km and floor elevations between −4,215 and −5,770 m below the Mars datum) were identified using a database of all Martian craters published by Robbins and Hynek (2012) and integrated with further observations. We focused on the northern hemisphere because this is where a large fraction of groundwater upwelling is predicted to have occurred (Andrews-Hanna & Lewis, 2011; Andrews-Hanna et al., 2007, 2010; Michalski et al., 2013). We selected craters with floor depths less than −4,000 m below the Mars datum; in particular, we selected craters below 37°N to limit ice noise or deposits associated with it, as the north cap reaches about 37°N at its maximum extent (Michaux & Newburn, 1972; Slipher, 1962). Furthermore, this was done to avoid confusion with landforms on Mars that are morphologically similar to terrestrial glacial and periglacial landforms occurring in the midlatitudes, between about 35°N and 60°N (Hauber et al., 2011, and references therein). Moreover, based on current surface conditions, the location of a subpermafrost groundwater table is presumed to occur below the subsurface melting isotherm estimated by Clifford and Parker (2001), which is <5 km at 30° latitude. We looked for evidence of intracrater fluvial activity and lacustrine deposits. In particular, we searched for locations where evidence of aqueous activity was present in the crater but absent in the terrain outside the crater (i.e., the crater was not fed by surface drainage, excluding short sapping valleys). As we wanted to investigate craters that have most likely formed during episodes of groundwater upwelling, prior to the Amazonian and Late Hesperian, we restricted our study to regions determined to be of Noachian to Early Hesperian age in the global stratigraphic chart recently updated by Platz et al. (2013) and Tanaka et al. (2014). Although crater-based absolute model age estimates for each of the 24 investigated craters could constrain the temporal occurrence of groundwater upwelling activity on Mars, we decided not to perform crater

Table 1
List of the Studied Craters

ID	Crater name	Latitude longitude	Diameter (km)	Floor elevation (m)	Crater depth (km)	Landslide (slump/debris flow/hummocky)			Sapping Valley	Delta (front elevation)
						Slump (e.g., El Hierro)	Debris flow	Hummocky terrain		
1	Nameless 1	27°54′19.36″N 11°29′42.67″E	69	−4,690	3.0	✓	✓	✓		✓(−4,000; stpd)
2	Pettit	12°15′8.64″N 173°51′58.60″O	92.49	−5,770	3.1	✓	✓	✓		
3	Sagan	10°43′22.75″N 30°36′11.55″O	90.26	−4,927	2.9	✓	✓		✓	
4	Nicholson	0°12′39.97″N 164°25′49.81″O	102.5	−5,124	3.1	✓	✓	✓	✓	✓(−4,200)
5	McLaughlin	21°54′28.66″N 22°21′16.17″O	90.92	−5,050	2.2	✓	✓			
6	Du Martheray	5°27′15.55″N 93°34′51.24″E	102	−4,753	2.3				✓	✓(−4,500)
7	Nameless (Du Martheray)	6° 6′10.31″N 94° 0′38.44″E	36.15	−4,575	2.1				✓	✓(−4,000/ −4,400; stpd)
8	Nameless 2	1°12′23.79″N 133°56′32.31″E	44	−4,215	2.7	✓(−4,000)				
9	Nameless 3 (in Trouvelot) ex candidate Mars rover landing site	15°53′2.15″N 12°44′59.28″O	28	−4,415	1.4	✓	✓	✓		✓(−4,000; stpd)
10	Nameless 4	15° 8′51.65″N 26°43′13.10″O	60	−4,275	2.4	✓				
11	Nameless 5	18°20′20.33″N 178°46′41.77″O	44	−4,912	2.2	✓	✓	✓	✓	
12	Nameless 6 (in Becquerel)	22° 5′3.78″N 8°15′17.00″O	53.8	−4,447	1.6					✓(−4,100)
13	Tombaugh	3°33′28.93″N 161°55′25.33″E	60.3	−4,542	2.2	✓	✓	✓	✓	✓(−4,300)
14	Nameless 7	12°19′50.23″N 34°31′1.21″O	68.5	−4,380	2.1					
15	Nameless 8	17°55′35.10″N 169°42′49.89″O	57	−5,103	2.0	✓	✓	✓		✓(−4,800, stpd)
16	Nameless 9	24° 2′59.53″N 177°20′54.00″O	46.3	−5,215	2.1	✓	✓		✓	✓(4,700; stpd)
17	Mojave	7°29′2.78″N 32°59′10.92″O	58	−5,190	2.6		✓(−4,600)			
18	Eden Patera	33°46′9.22″N 11° 3′26.75″O	52	−4,990	2.8	✓			✓	✓(−4,300)
19	Nameless 10	31°26′37.37″N 12°55′55.55″O	40.1	−5,167	2.2	✓	✓	✓		✓(−4,500; stpd)
20	Curie	28°46′59.38″N 4°45′2.88″O	114.1	−4,547	2.3	✓(−4,000)	✓	✓		✓(−4,300)
21	Nameless 11	10°13′3.21″N 94°18′16.00″E	45.4	−5,200	2.5	✓(−4,000)	✓	✓		✓(−4,200)
22	Oyama	23°33′58.32″N 20° 6′43.20″O	100	−4,358	2.1					✓(−4,100)
23	Wahoo	23°14′0.36″N 33°40′53.76″O	62	−5,091	2.0	✓(−4,200)	✓	✓		✓(−4800)
24	Nameless 12	15°23′22.17″N 178°26′21.82″O	64.2	−4,520	2.1	✓		✓	✓	

Note. Stpd = stepped; CRISM = Compact Reconnaissance Imaging Spectrometer for Mars; HRSC = High Resolution Stereo Camera; DEM = digital elevation model.

Table 1 *(continued)*

ID	Channel (base elevation)	Shoreline (elevation)	Fan (front elevation)	Inverted morphology	Flat floor	Mineralogy/ sedimentology	CRISM/HRSC DEM	Depositional inner crater slope	Floor slope	Delta surface (km^2)/volume (km^3)
1					✓	Possible Phyllosilicates on fan (to check in detail)	Yes/No	20%	0.32%	2.96/0.59 -2.65/0.53 -9.44/2.36 -6.88/1.38
2					✓		Yes/Yes	20%	0.26%	
3	✓(−4,200)	✓(−4,600)	✓(−4,300)	✓ (Starting from −4,500)	✓		Yes/Yes	12%	0.09%	
4	✓(−4,200)	✓(−4,000)			✓		Yes/Yes	25%	0.27%	1/0.1
5	✓ (−4,200 start −4,700 end)		✓(−4,400)		✓(partially)	Clays + Carbonates	Yes/Yes	24%	0.30%	
6	✓(−4,000)	✓(−4,000 and −4,400/ −4,500)			✓	Possible Phyllosilicates	Yes/No	11,5%	0.16%	
7					✓	Sedimentary deposits (floor)	No/No	12,5%	0.28%	31/2.48
8					✓	Possible Phyllosilicates Light toned layered deposits on the floor	Yes/No	14%	0.21%	109/3.27
9		✓(−4,200)			✓	Light toned layered deposits (floor)	No/Yes	33%	0.24%	3.86/1
10	✓(−4,000)	✓(−4,000)			✓	Layered deposits (floor)	No/Yes	18%	0.19%	
11	✓(−4,600)	✓(−4,000 −4,700)	✓(−4,400)		✓		No/No	25%	0.12%	
12		✓(−4,250)			✓	Layered deposits (floor)	No/Yes	21%	0.05%	9.35/1.87- 1.91/0.28
13	✓(−4,400)	✓(−4,400)			✓		No/No	11%	0.32%	5.31/1.06
14	✓(−4,200)			✓	✓	Layered deposits (floor)	No/Yes	15%	0.01%	
15	✓(−4,400)	✓(−4,400)			✓	Layered deposits (floor)	No/No	11%	0.18%	8.29/2.49- 4.9/0.68
16	✓(−4,700)	✓(−4,700)	✓(−4,700)	✓(Starting from −4,700)	✓	Layered deposits & erosional windows (floor)	Yes/No	14%	0.12%	2.6/0.1
17			✓(−4,600)		✓		Yes/Yes	20%	0.11%	
18	✓	✓			✓(partially)		No/Yes	30%	0.26%	0.33/0.13
19				✓	✓(partially)		No/No	28%	0.07%	6.4/2.51
20	✓(−4,400)	✓(−4,400)			✓	Layered deposits	No/Yes	14%	0.14%	2.25/0.16
21	✓(−4,700)				✓		Yes/No	20%	0.35%	0.37/0.008
22	✓(−4,000)	✓(−4,000)			✓(partially)	Clay-rich layers and layered deposits on the floor	Yes/Yes	14%	0.07%	1.04/0.11
23	✓(−4,600)	✓(−4,300 and −4,600)	✓(−4,500)		✓	Possible Phyllosilicates (floor) Layered deposits	Yes/Yes	17%	0.2%	0.35/0.07
24			✓(−4,300)		✓	Remnant of megaslump on the floor	No/No	28%	0.12%	

counts due to little prospects of deriving reliable age data. The reasons for our decision are explained in detail in the supplementary material. The identified 24 craters that fulfill our requirements are listed in Table 1.

3. Results

A conceptual model that describes the evolution of the upwelling and retreating groundwater levels in deep enclosed basins is proposed in Figure 2. It represents the evolution of the groundwater table level from a flooded crater in Stage 1 to a completely dry crater in Stage 3. The model is supported by satellite images where associated water-formed features (described in the following sections) are observed (Figure 3), and they testify to this evolution. The images show the following morphologies: sapping valleys, deltas, channels, terraces, gravitational collapses with plastic behavior, alluvial fans, and exhumed channels.

The studied basins show different stages of evolution, probably due to different porosity/permeability values of the substratum. The well-developed basins, where permeability/porosity is high, were characterized by long-lasting standing bodies of water and show almost all of the previous listed morphologies. The basins with lower permeability/porosity values exhibit only some of the previous listed morphologies as a result of the shorter duration of the lacustrine activity/phase.

The model (Figure 3) consists of three chronological stages that describe the landforms produced inside the well-developed basins due to groundwater upwelling and the subsequent drop in water levels until they became dry in the third and final stage of the model. In the first stage the crater was flooded and as a consequence sapping valleys with deltas, terraces, shorelines, and channels formed. During the second stage, possibly due to processes of percolation and/or evaporation, there was a net drop in water levels (although there may have been a number of higher-frequency water level fluctuations) and, consequently, new landforms were created. Deltas that were formed in Stage 1 were carved, and new channels and deltas were formed at lower levels; landslides occurred, and new shorelines were formed. Before the basins became totally dry, there was fluvial activity on the basins' floors where small channels and alluvial fans developed. In the final stage the crater became dry and exposed exhumed channels on the craters' floors as well as all the landforms developed in the previous two stages.

3.1. Deep Martian Sedimentary Basins and Associated Landforms

The analysis of the sedimentary basins at CTX (6 m per pixel) and where available at HiRISE (25 cm per pixel) scale allowed us to propose an interpretation of their geological history and in particular the role that groundwater could have played in the observed formations.

Deep basins are, in particular, the most appropriate candidates to investigate the geological history because, due to eolian erosion, the sedimentary record in shallower basins is often undetectable. Furthermore, in the case of a one-plate planet such as Mars (Banerdt et al., 1982; Breuer & Spohn, 2003), impact craters are among the few natural phenomena that are able to deform the surface (Ruj et al., 2017) and act as sedimentary basins with considerable and well-developed steep slopes (see Table 1 for crater walls' slopes). Erosional processes occurred on the basin walls creating sediments that accumulated within the basin, which acted as a terminal sink. During early Mars, widespread shallow lakes occupied the basins shown in Figure 1 (Fassett & Head, 2008; Goudge et al., 2015; see also Table S1 in the supporting information). Water-related morphologies and sediments can be easily observed today in these basins and they form an important reference point with which to measure the putative depth of a global groundwater table. Since these basins are enclosed and isolated from surface runoff from the plateau, it is likely that all of the water-related processes within the craters are due to groundwater activity. All 24 basins are located along the dichotomy boundary and many of them are clustered in the Arabia and Amazonia quadrangles along two parallel lines aligned NNE-SSW in the first location and NNW-SSE in the second (Figure 1). In the following subsections we describe the water-related morphologies in the studied basins and explore their connection with groundwater activity. An overview of all of these morphologies is also available in Table S1 (supporting information).

3.1.1. Valleys

Several craters walls show steep (e.g., 25%) valleys with amphitheater-like headwalls, roughly uniform widths, and abundant evidence of mass wasting (Figures 4a, 5a–5c, 6d and 6f, 7, and 8c). These valleys lack a visible upstream channel for water supply and sometimes they cut through a crater rim, which indicates

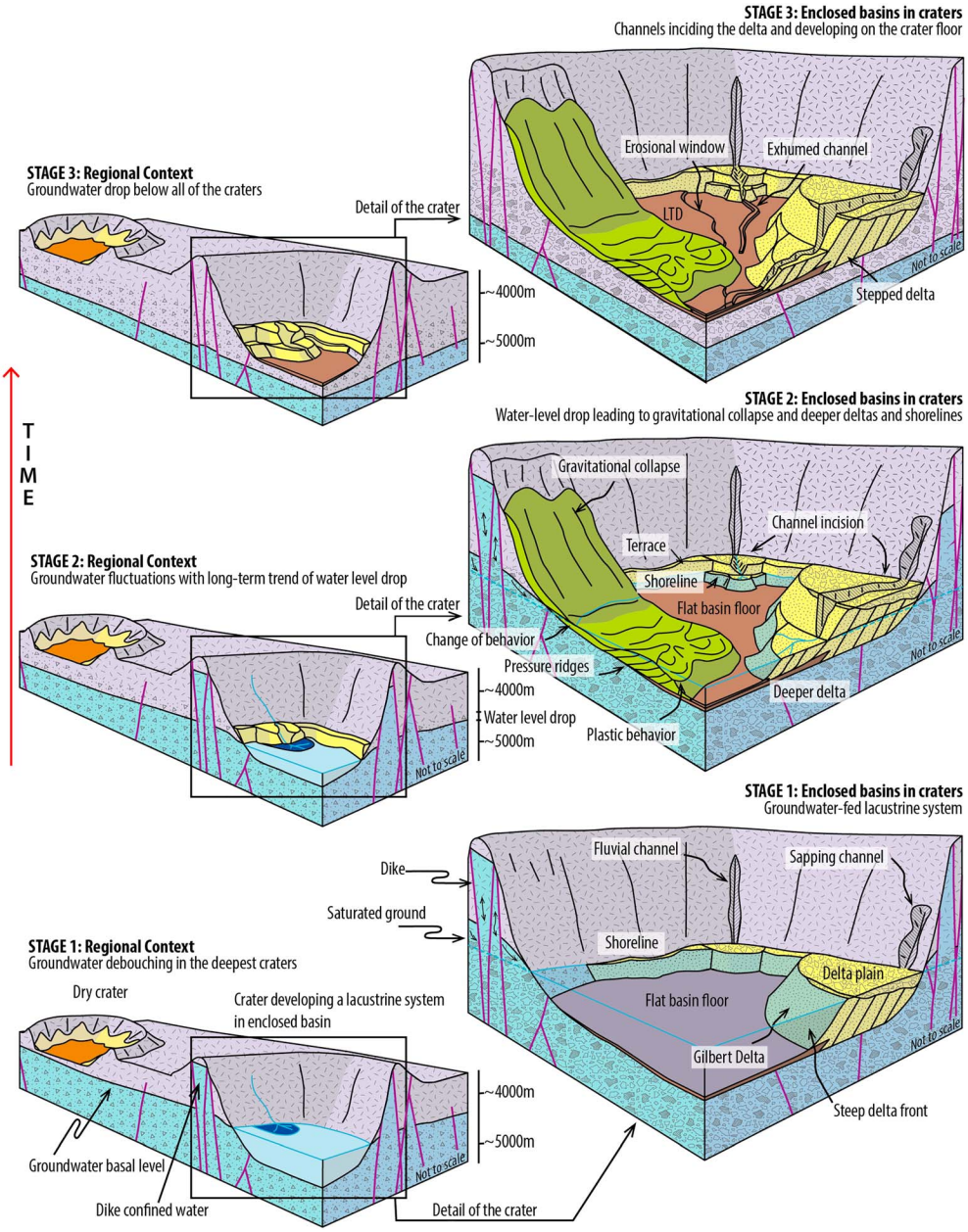

Figure 2. Conceptual model, of Martian basins evolution and their relations with the groundwater storage, from the oldest (bottom) to the most recent stage (top). The model consists of three chronological stages. In the first stage, the crater was flooded and as a consequence sapping valleys with deltas, terraces, shorelines, and channels formed. During the second stage, there was a net drop in water levels (although there may have been a number of higher frequency water level fluctuations) and new landforms were created as a consequence of this process. In the final stage the crater became dry and exposed exhumed channels on the craters' floors as well as all the landforms developed in the previous two stages. This model also introduce for the first time in the Martian geological literature the possible presence of "dike confined water" that can make the groundwater level shallower than the basal one, allowing the formation of sapping valleys and other water related morphologies even if, for instance, the groundwater basal level is deeper than the head of the sapping valleys (see also section 4.1, and references therein).

that they were formed by headward erosion. They show low-drainage density, a paucity of downstream tributaries, and flat valley floors with constant width or widening in the headward direction. Most of them end with fan-shaped deposits at their mouths. Furthermore, they do not show evidence of inner channels or small-scale tributaries.

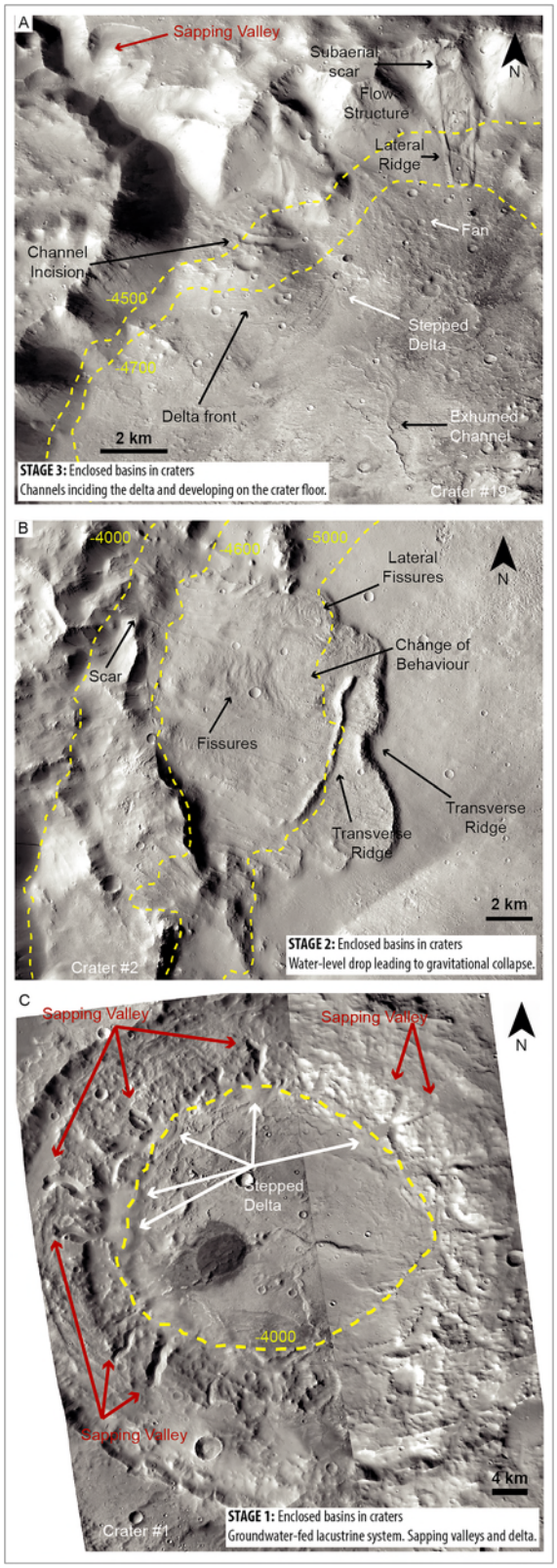

Figure 3. Satellite images showing morphologies that support the conceptual model. The images (a-c) show the following morphologies: sapping valleys, deltas, channels, terraces, gravitational collapses, fans, and exhumed channels.

Interpretation: Amphitheater-like headwalls are characteristic of sapping valleys and outflow channels. However the characteristics of the studied channels are inconsistent, due to their morphometry, scale, and association with other landforms formed as outflow channels, suggesting that these morphologies might represent sapping valleys.

3.1.2. Channels

The studied basins show evidence of channels carved in the crater walls (Figures 6, 8d, and 9b). The channels do not reach nor breach the crater rim, and it is notable that their lower sections are located at roughly the same elevation. They are shallower, narrower, and do not present amphitheater-like headwalls. For instance, in Figure 9b they cover the inner part of the crater wall. The channels generally terminate in correspondence with a broad platform (Figure 4b) or at the craters' flat floor. These channels are shown, for example, in Figures 6d and 6e where the differences with the putative sapping valleys are emphasized.

Interpretation: The base of these channels define a sort of "equipotential" surface and thus constitutes a kind of "marker morphology," because it implies a common base level which in turn suggests the presence of a standing body of water.

3.1.3. Terraces

The inner part of the crater wall is often encircled by broad platforms. Although rarely continuous, they spread laterally at a near horizontal elevation (e.g., Figures 3c, 4b, and 10). These platforms have enough topographic expression to be defined on HRSC-derived digital elevation models. Accordingly, we interpret them as terraces/beach deposits formed in standing water (Ori et al., 2000; Ori & Mosangini, 1998). We discarded the hypothesis that these terraces could be part of the original crater shape both because these craters are not fresh enough to eventually preserve it (Robbins & Hynek, 2012) and because most of them show the same topographic elevations of other putative water-related morphologies (e.g., channels).

3.1.4. Delta

Fifteen of the 24 enclosed deep basins show dark-toned, arcuate-shaped features in plan view (Figures 4, 6c, 7b and 7d–7f, 8b, 9c, and 10) radiating from a channel, sometimes showing an irregular perimeter and an elongated planimetric pattern with channel-incised lobes. They also present a near flat (about 1%) radial profile on their surfaces and a steep front (see some examples of topographic profile in the supporting information). Some of the investigated features show stair-stepped morphologies (e.g., Figure 4c). Based on a combination of CTX and HRSC/MOLA digital elevation model data, we calculated the surface and volume of these deposits (Table 1) using the "surface volume" ArcGIS 10.6 tool.

Interpretation: We interpret these fan-shaped morphologies as typical Gilbert-type deltas (Gilbert, 1885; Ori et al., 2000; Postma, 1990), which were formed during periods when the water level in the crater was stationary. Some show stepped retrograding deltas that were formed during periods of rising water levels (e.g., Figure 4c), while in others the presence of incised deltas constitute evidence of dropping water levels. Some of the studied fan deltas, such as the one in Figure 4c, present radiating inverted channels on their surfaces and a steep scarp, which we interpret as a delta plain and delta front respectively. The presence of inverted channels and delta fronts suggests that at times the standing water table reached at least the topographic elevation corresponding to the transition between these

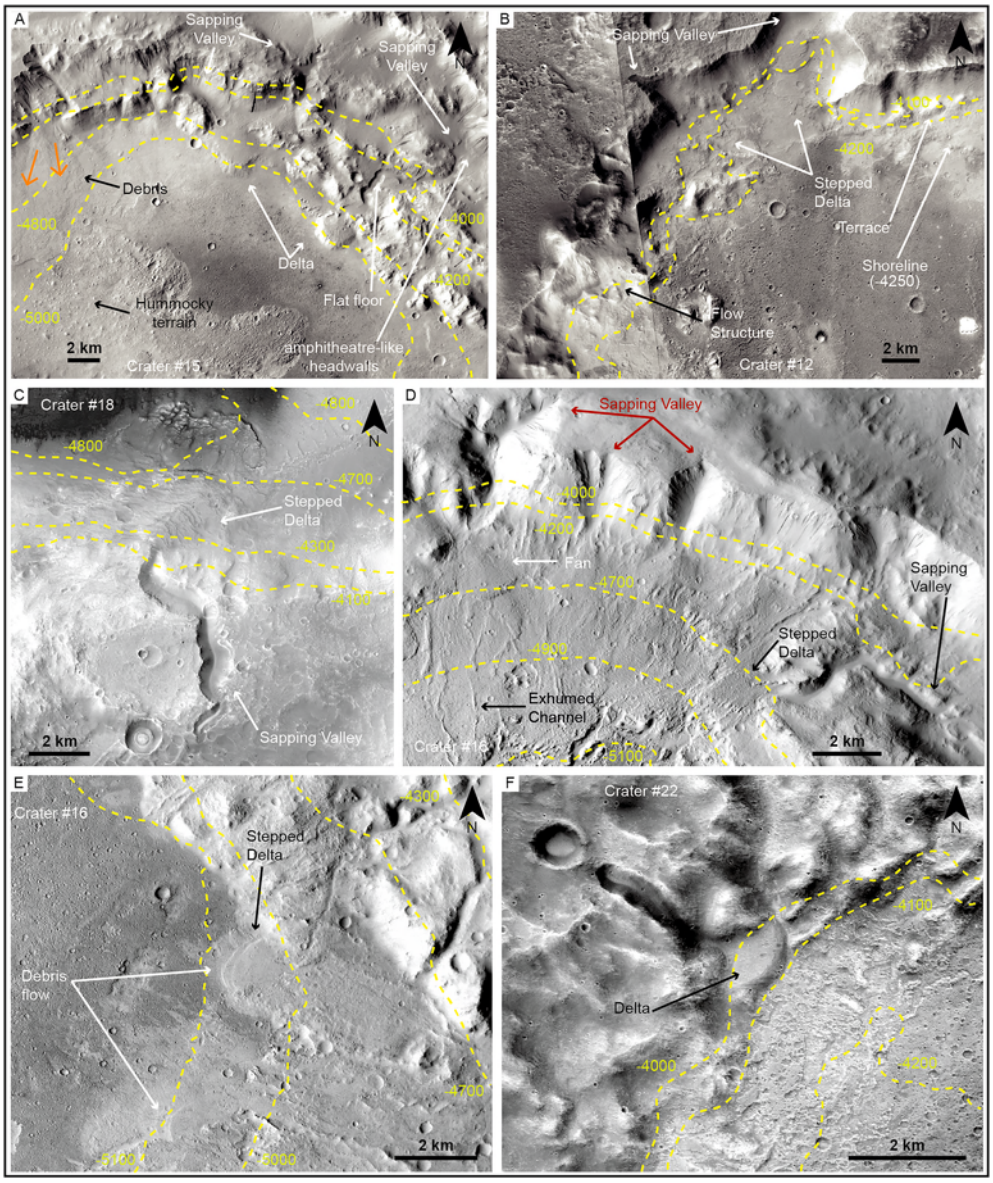

Figure 4. Morphologies inside several basins. (a) Crater #15 shows the presence at the same time of delta, sapping valleys, debris, and hummocky terrain. The basin floor is flat. (b) Crater #12 shows stepped delta, terraces, shorelines, and flow structures at roughly the same topographic elevations. (c) Sapping valley and related stepped delta in crater #18. (d) Sapping valley and related stepped delta along with fan and exhumed channels in crater #12. (e) Crater #16 shows well-preserved outcrops of debris flow. (f) Sapping valley with related delta at −4,100 m inside crater #22.

environments. We also note that post depositional eolian abrasion probably scoured the finer-grained part of these fan delta deposits. This evidence is consistent with the other water related morphologies in Figure 4c, where the crater floor deposits might be of lacustrine origin. The presence of fan deltas sourcing from the basin wall, either stepped or not, is documented in at least 15 basins, sometimes with several fan deltas in the same basin (e.g., Figures 3, 4, 7, and 8).

3.1.5. Cone/Alluvial Fan

In some craters the mouths of short fluvial channels develop into radial length fan-shaped landforms (Figures 3a and 4d), which in several cases present a semiconical form, a branching tributary network, distributary channels, and incised channels (e.g., Figures S6 and S13). Moreover, they present a concave-up, gently sloped, profile in the longitudinal profile and a concave-up profile perpendicularly to the flow direction (e.g., Figure S14).

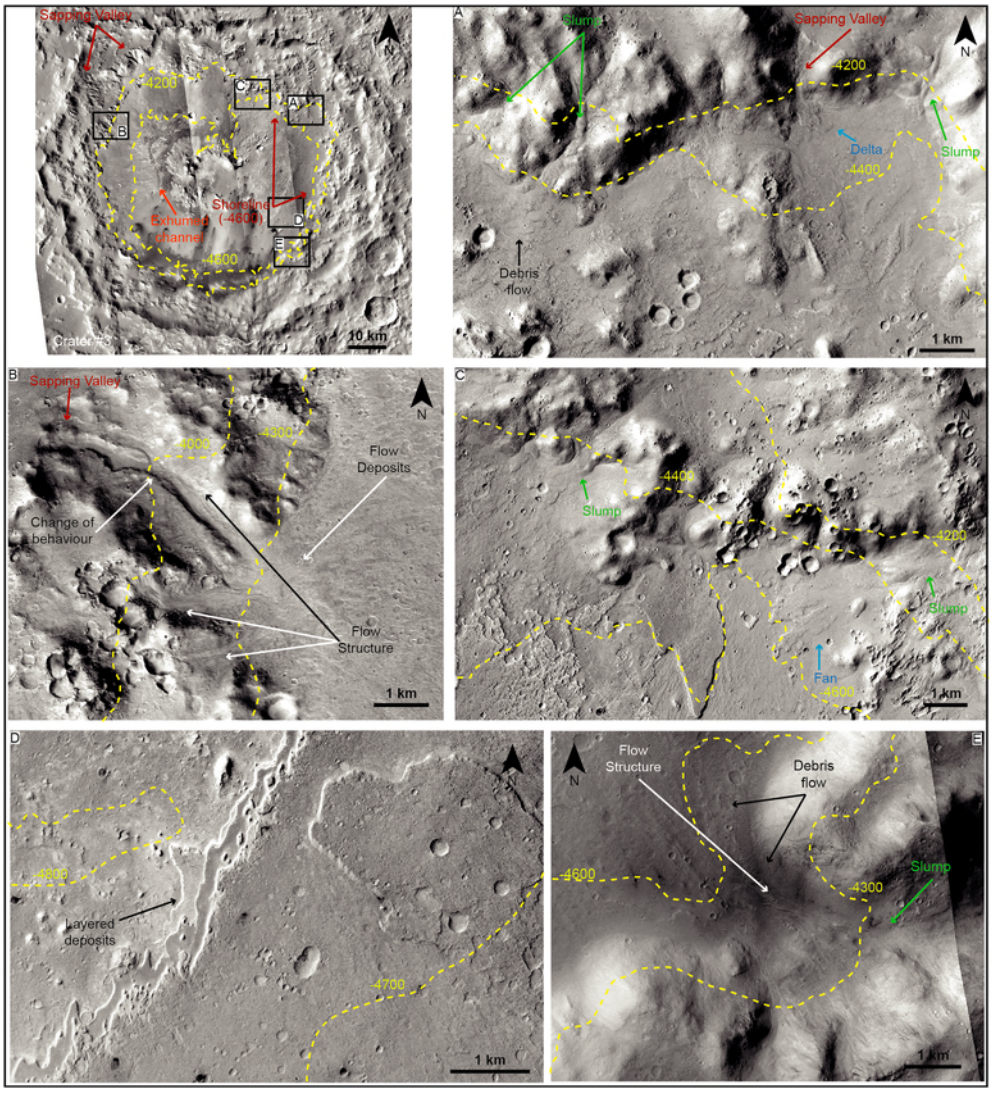

Figure 5. Morphologies inside Crater #3 with contour lines (yellow). (a) Several slumps (green) and a sapping valley (red) with a delta (blue). Large debris flows across the crater floor. (b) Sapping valleys and flow deposits. (c) Sapping valley and flow deposits across the crater floor. (c) Slumps (green) and a large fan deposit. (d) Layered deposits on the crater floor. (e) Slump followed by a flow structure and debris flows.

Interpretation: These morphologies are already well studied both on Earth and Mars. Based on the above mentioned criteria, they can be interpreted as alluvial fans due to the absence of evidence showing interaction with features that suggest a standing body of water. Nevertheless, on Earth, very young and immature deep-water systems may be characterized by a "bypass" slope and they can represent debris cones (Postma, 1990; Prior, 1988). These deposits superpose the uppermost basins flat floor and the layered bed in the studied basins suggesting a late stage emplacement and a progressive drop of the water table. The nomenclature dilemma (Cone/Alluvial Fan) is due to the fact that the morphological criteria used to distinguish between the two morphologies in modern systems is difficult to apply to the fossil environments.

3.1.6. Crater Floor

Crater floors are generally smooth, flat, or partially flat (see Table 1 for slope values), and they are sometimes characterized by the presence of erosional windows and LLDs. The layered deposits are present at the base of almost all the inner rims and they shallowly slope toward the basin's center.

Interpretation: The flatness of the surfaces could be partly inherited by the geometry of the crater but possibly enhanced by fine-grained sediments that draped and smoothed the underlying topography. Such

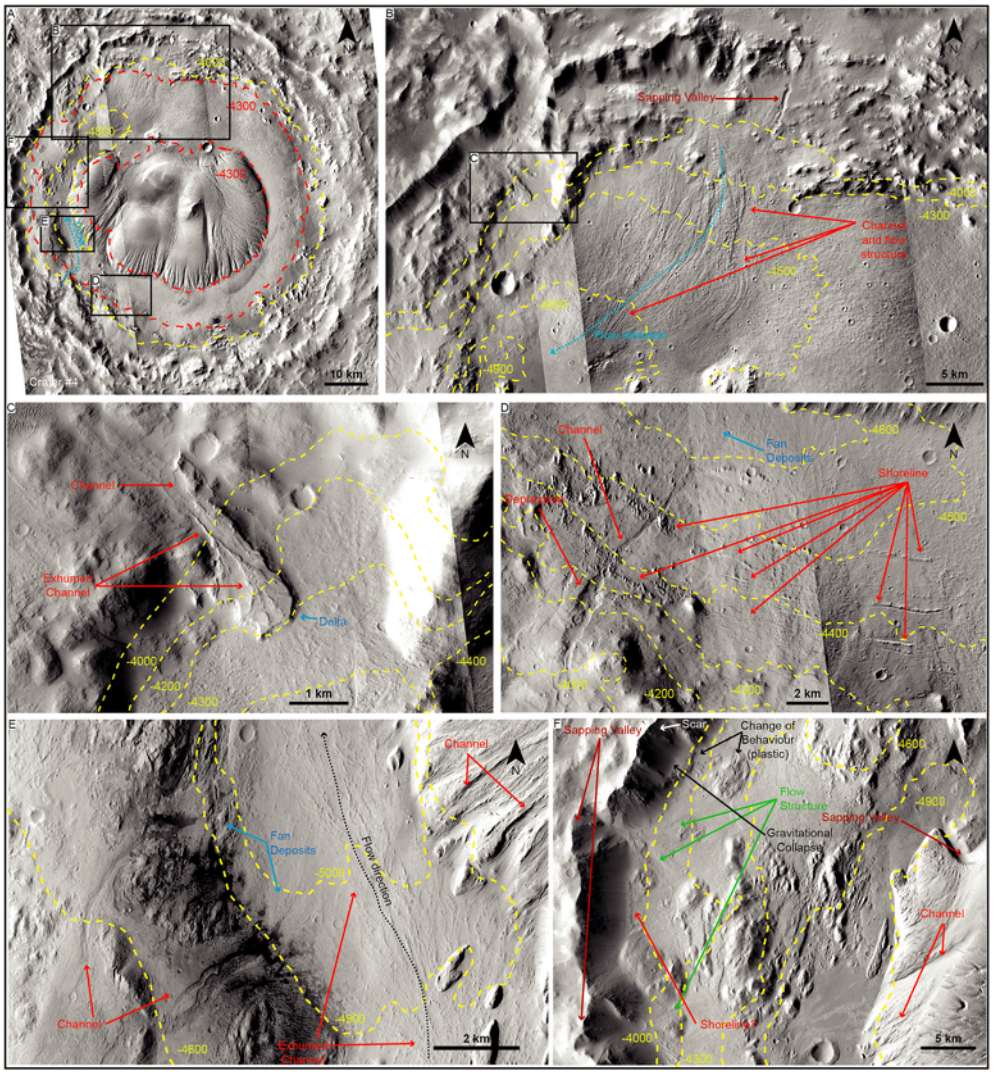

Figure 6. Morphologies inside Crater #4. (a) Location image with contour lines in red and yellow. The red line marks the elevation of −4,300 m, which represents the base level of several water related morphologies on the crater wall as well as on the central mound. (b) Sapping valley and large flow structure with channel. Flow direction to the southeast (blue line). The flow structure suggests a progressive fall in the water level; in fact, these structures converge toward the deepest part of the basin and this is consistent with decreasing water levels. (c) Channel transitioning to an exhumed channel terminating with a remnant of delta front at −4,200 m. (d) Large channel with fan deposit. Possible remnants of shorelines observed perpendicular to the channel and concentric with the crater wall. The evidence of shorelines and a fan are consistent with the flow structure in panel b, both converging toward the deepest part of the basin showing the basin's late life stage. (e) Channels and associated fan deposits. A possible exhumed channel observed on the floor. Flow direction on the floor to the north (black line). Again, flow direction is opposite to that of those in panel b, this evidence corroborates our hypothesis about the late stage water level decrease in this basin. (f) Landslide scar, several sapping valleys and channels (red). Flow structures observed on the floor (green). All the morphologies below −4,000 m are consistent with a wet environment.

depositional geometry is consistent with settling of sedimentary material (i.e., landslide-driven or delta-fed distal turbidite deposits).

3.1.7. Landslide

Sixteen of the studied craters show near-vertical amphitheater-shaped headwalls on the crater rim, a detachment niche (scar) on the upper part of the crater slope, and a pile of avalanche debris at the foot of the steeper crater slopes (Figures 3, 5, and 8). The material from the scar came to rest at the head of the slide, while the material from the lowermost part of the source area came to rest at its toe. Slides have fanlike shapes where they move out over the crater floor and their deposits are thin compared to their lengths. Lateral and distal

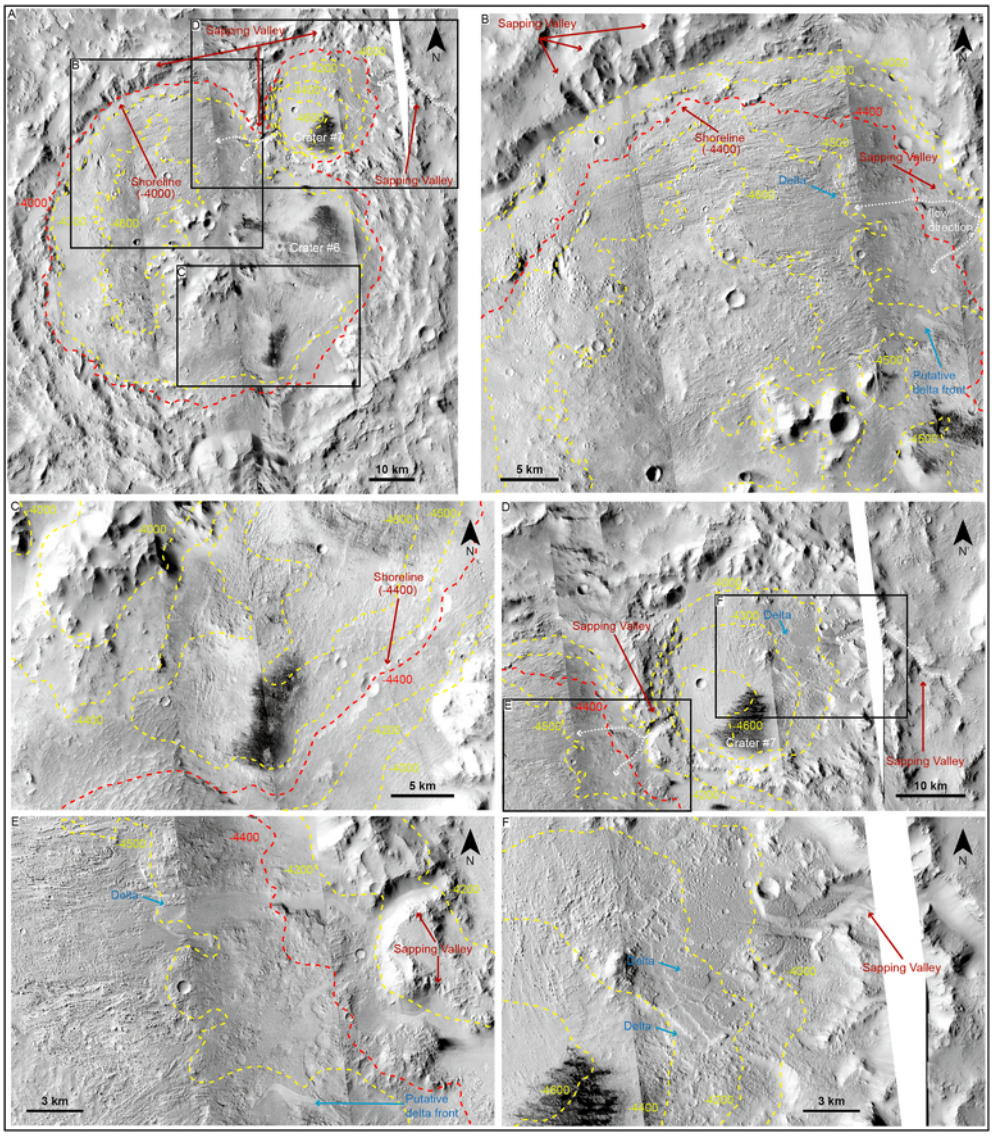

Figure 7. Morphologies inside Craters #6 and #7. (a) Location image with contour lines in red and yellow. The red contour line marks the elevation of −4,000 m. White lines indicate flow from Crater #6 into Crater #7. Red contour line (−4,000) is "open" among the craters and coincides with the base of sapping valleys in both craters and with the shoreline. Furthermore, −4,000 m is also the elevation of the top of the channel between crater #6 and crater #7. Contour lines start to be closed in those craters from −4,200 m. (b) Sapping valley and possible shoreline marked by −4,400-m red contour line. Deltas observed at the end of a flow channel from Crater #7. (c) Observed shoreline in the southern edge of Crater #7. (d) Locations of e and f. We can clearly observe the −4,000-m contour line; most probably a standing body of water filled these two craters up to this elevation as is also testified by the delta front in crater #7. Then the water level dropped and a breached happened in the SSW part of crater #7 draining part of the water into crater #6. The latter crater also presented a standing water table, as testified by the presence of a delta front (following panel). (e) Sapping valleys with deltas. (f) Sapping valley and two deltas in Crater #7. Delta deposits at the mouth of the sapping valley are carved until about −4,300 m.

rims form distinct ridges (Figures 8a and 8b). Landslide deposits in these deep basins generally display a change in behavior, becoming more plastic and displaying flow structures in the lower parts (Figures 3, 4, and 8). It is noted that the level where this change of behavior occurs is the same as the level of other water-related morphologies and/or deposits (e.g., fluvial delta and shoreline), which reinforces the idea of the existence of a stationary water level. The landslide deposits consist of massive debris at the head and hummocky deposits farther out.

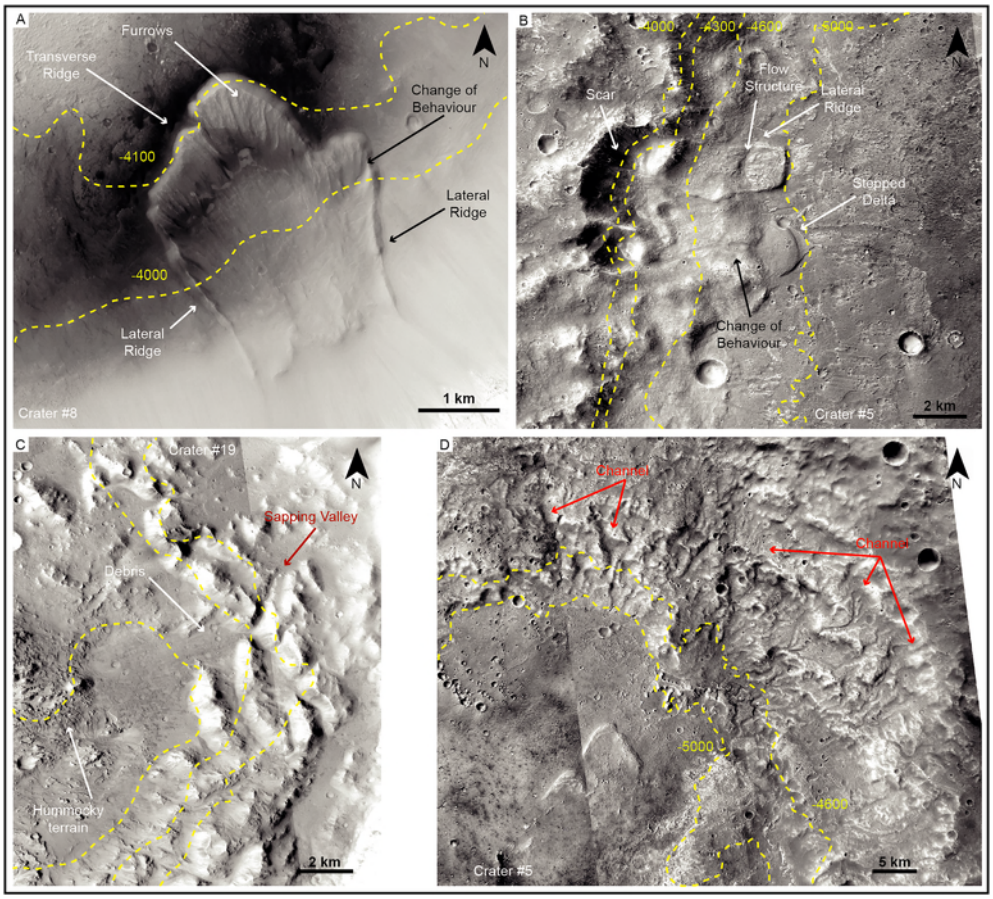

Figure 8. (a and b) Well-preserved examples of gravitational collapse with plastic behavior below −4,000 m. (c) Sapping valley, debris flow and hummocky terrain inside Crater #19. (d) Channels ending around −4,700 m in Crater #5 testifying putative water standing body at this elevation.

Interpretation: We interpreted these large accumulations of debris, which can be seen in several of the craters analyzed (Table 1), as the cumulative result of several landslide processes where slumps, debris flows and hummocky terrains are all present.Landslides identified in this study show a variety of structures that suggest elements of both debris avalanche and debris flow emplacement mechanisms. It would be possible to image and investigate those fine textures and facies with HiRISE, but its spatial coverage is limited and the image resolution of CTX data used in this study is not adequate to establish the texture and facies of the deposits. These landslides can also initiate turbidity currents, which are capable of flowing considerable distances downslope and might explain the flat floor morphology even if available data does not allow the recognition of sedimentary texture and structures to constrain such a hypothesis.

In analogy with Earth (Masson et al., 2006; Weaver et al., 2000) these landslides could have occurred in a wet or partially wet environment or in areas where fine-grained sediments, sometimes clay rich, are present (e.g., area of Mc Laughlin and Oyama craters; Loizeau et al., 2012; Michalski et al., 2013). On Earth, a debris flow can be triggered when there is more than 10% of clay among the sediment. Here, the fine-grained material might be the weathering product of altered crater material.

3.1.8. Inverted Morphologies

We observed inverted morphologies on the crater floor and in the lower part of the walls of some basins, which we interpreted as exhumed channels (Figures 4a and 8d). These channels were formed at the final stages of the basins when they were still in a wet condition, as shown by crosscutting relations and relative stratigraphy (e.g., Figure 4a). They were later exhumed due to the lowering of the landscape through denudation processes such as mass wasting, fluvial dissection, or eolian deflation, leaving the more indurated parts as ridges in the landscape, and thus inverting the former topography (Pain & Ollier, 1995).

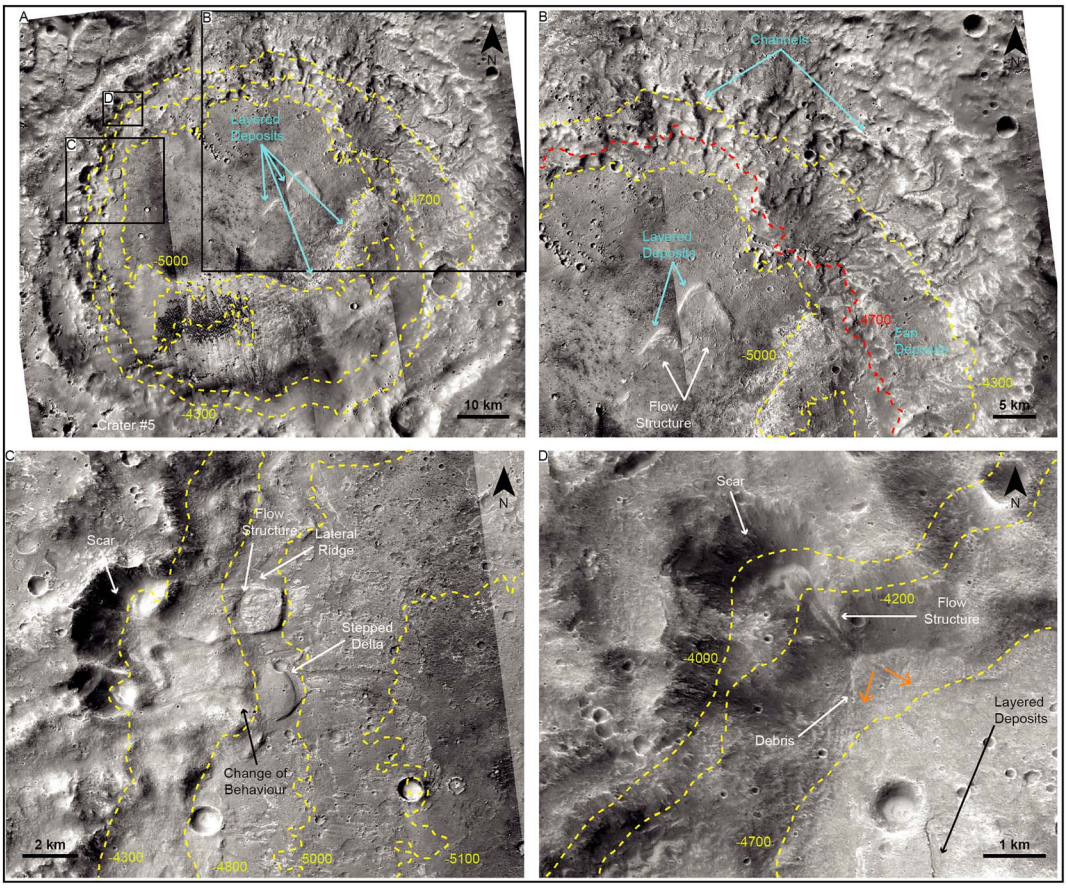

Figure 9. Morphologies inside Crater #5. McLaughlin crater presents water related activity starting around −4,300 m, and at least one stage of water standing body around −4,700 m as testified by the morphologies indicated below. (a) Location image with layered deposits (blue) and contour lines. (b) Channels and fan deposits with a large layered flow structure in the center. (c) Landslide scar on the east side of the crater with associated flow structure and lateral ridge. A stepped delta can also be observed. (d) Landslide scar and associated flow structure and debris. Orange arrows indicate flow direction.

4. Discussion

The simultaneous presence of a variety of water-formed features such as sapping valleys, deltas, channels, alluvial fans, landslides, flat floors, and exhumed channels are all found in close association in the studied craters. Taken together, these landforms suggest a formation in fluviolacustrine depositional settings. We further note a consistent range of elevation for all of these morphologies, as shown in Table 1 and particularly in Figure 11, which allows us to infer an associated (although fluctuating) water level.

What emerges from Figure 11 is that most morphologies (including delta) oscillate between −4,000 and −4,500 m, which is a notably limited range given the distribution of various sites throughout the northern equatorial hemisphere. For some craters the symbols in Figure 11 overlap each other to indicate that those morphologies in that site are at the same elevation.

The study, and in particular the holistic consideration of all these laterally related morpholiges in a landscape containing different depositional environments, supports the idea that in the past these craters contained water that progressively receded leaving behind landforms in a specific chronological order. Nevertheless, our research still leaves some questions open, which we will discuss below, including the following: Is seepage or is water flow erosion the more likely mechanism for valley formation? Is there any inconsistency between the lack of sediment in the deep basins and groundwater upwelling? What was the main control on deposition, groundwater and/or precipitation?

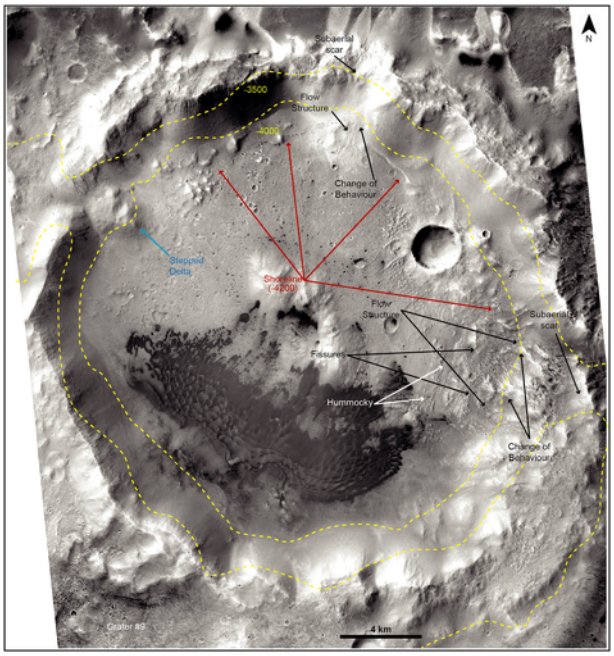

Figure 10. Morphologies inside Crater #9. A large stepped delta can be observed on the northeast side of the crater. Possible shoreline indicated at −4,200 m (maroon arrows).

4.1. Sapping Valleys Genesis

The distinction between seepage and water flow erosion in valley formation is subtle. The valleys analyzed in this work have roughly uniform widths and show steep amphitheater heads. According to Sharp and Malin (1975), amphitheater-headed valleys are a common indication of groundwater-seepage erosion and, more recently, Harrison and Grimm (2005) interpreted these valleys as markers of an increased relative contribution of groundwater to erosion from the late Noachian into the Hesperian period. Nonetheless, other formation mechanisms of these valleys cannot be excluded on the basis of their morphology alone. Several mechanisms such as groundwater seepage (Goldspiel & Squyres, 2000; Howard, 1986; Kochel & Piper, 1986; Malin & Carr, 1999; Schumm et al., 1995), overland flow (Lamb et al., 2008; Lapotre & Lamb, 2018), and combinations of the two (Amidon & Clark, 2015; Laity & Malin, 1985; Pelletier & Baker, 2011) have been suggested to explicate the genesis of amphitheater-shaped valleys both on Earth and Mars.

Pelletier and Baker (2011) applied numerical models to show that amphitheater headwalls are diagnostic of seepage erosion. Nevertheless, more recently Lapotre and Lamb (2018) proposed that valley formation by seepage erosion can only occur in sand because of its relatively unique mobility and permeability properties, which is consistent with experimental observations (Howard & Mclane, 1988; Marra et al., 2014). In competent rock, the authors find that a more plausible scenario for large valleys is erosion by overland water flows.

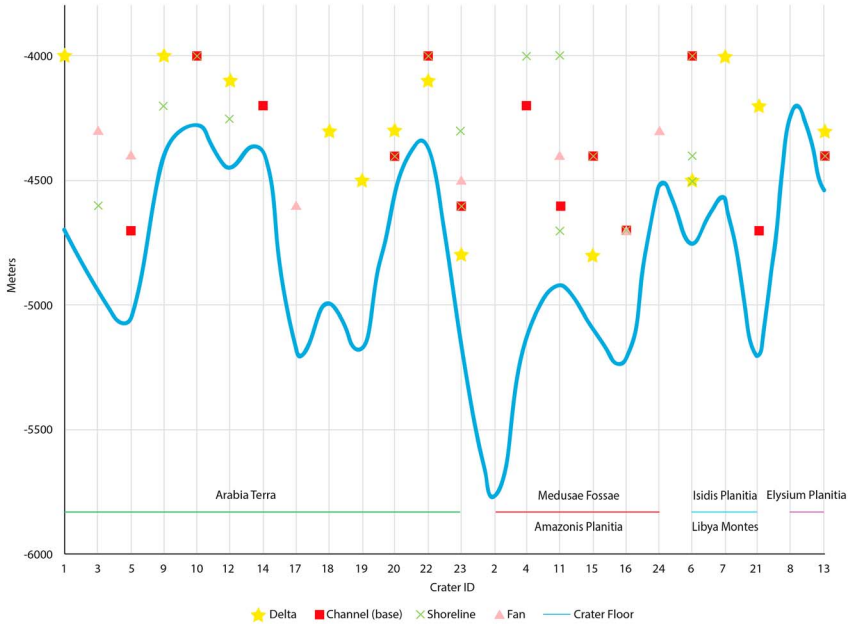

Figure 11. Elevations of most of the morphologies described in the main text and listed in detail in Table 1. The *X* axis shows the crater ID as in Table 1, and the *Y* axis shows the elevation in meters. Most of the morphologies are between −4,000 and −4,400 m and in several cases they are superposed in the diagrams, indicating that they occurred at same elevation in the same basin. The solid line represents the elevation of the crater floors. This diagram synthetizes the purpose of this work: Our aim is to consider all of these water related morphologies holistically and in a planetary-wide scale. Except for the delta top, which gives us a confident estimation of the water level within the basin, in some cases the morphologies present different elevations within the same basin; this is due to the fact that they register the last stage of life of these basins. Morphologies developed at different stages, registering the water level fluctuations and/or drop.

Lapotre and Lamb (2018) while reporting in their paper evidence of groundwater-seepage valleys engraved in the volcanic bedrock, they ignore terrestrial field evidence of groundwater upwelling and sapping valleys carved in volcanic consolidated deposits such as those reported by several authors (Izuka et al., 2018; Kochel & Piper, 1986; Macdonald et al., 1983; Stearns, 1966).

Porosity and permeability drive the groundwater occurrence and movement within rocks. Basalts generally have moderate porosities (10–30%) but include some of the most permeable formations on Earth (Macdonald et al., 1983). Basalt's permeability is mostly due to its internal structures such as clinker layers in "aa" lava, lava tubes in pahoehoe, irregular openings between flow surfaces, gas vesicles, and vertical contractions joints formed by cooling lavas (Peterson, 1972).

On Earth, such as in Hawaii, for example, sapping valleys form even when the basal groundwater does not reach the valleys' head. This is due to two different processes, the so-called "high level groundwater" and the more important "dike-confined water" (Izuka et al., 2018; Macdonald et al., 1983). The high-level groundwater forms when the descending water reaches an impermeable bed (perched groundwater) such as dense lava or volcanic ash. Where erosional valleys cut across the perching members, the perched water may run out.

In the presence of numerous dikes, which constitute nearly vertical and less permeable walls, the water accumulates in compartments of more permeable rocks between the dikes as it rises in level. In some dike complexes on Earth, water is held between the dikes to a height of more than 600 m. This is the case of dike-confined water, more relevant for the Martian case (see Figure 2 for graphical explanation; please compare to terrestrial field example by Macdonald et al., 1983, Figure 11d). The valleys that tap these aquifers incise at accelerated rates compared to valleys fed only by runoff. Sapping valleys evolve by gradual headward growth, maintaining a steep theater head. Sapping valleys combined with efficient fluvial transport in the channels can accumulate sediment at their mouth (Kochel & Piper, 1986).

It is very likely that the hidden Martian stratigraphy is mainly composed by basaltic lava flows, favoring the presence of dike-confined water as well as "perched water." Evidence of Martian Hesperian age basaltic lava flows associated to subvertical (cooling) joints carved by valleys were already shown by Mangold et al. (2008), and the deep Martian stratigraphy is still unknown.

Since only a few valleys on Earth (e.g., Schumm et al., 1995) are thought to be affected exclusively by seepage erosion (e.g., Lamb et al., 2006) and the component of water flow erosion cannot be excluded, we believe that a composite discharge model is a plausible formation mechanism for the amphitheater-headed valleys studied in this work. There is no evidence of large surficial floods in the intercrater plains around the craters or of flows cutting the craters from outside, as also suggested by Amidon and Clark (2015). Furthermore, a composite discharge model (overland flow and groundwater) is also consistent with the model proposed by Andrews-Hanna et al. (2007, 2010) and terrestrial field observation (Kochel & Piper, 1986).

The composite discharge model for amphitheater-headed valleys also has important implications for the Martian hydrologic cycle. It implies that valleys could be formed by groundwater discharge on a more rapid time scale than required by a seepage weathering mechanism (Lamb et al., 2006). It also suggests that the lower latitude valleys studied in this work could potentially be attributed to groundwater recharge or from nearby craters (Amidon & Clark, 2015).

4.2. Lack of Sediment Inside Deep Basins

The lack of sediment does not imply lack of geological events: stratigraphic record is "msore gap than record," as famously stated by Ager (1981) and agreed by (Dott, 1983). Especially within a hydrologically closed basin the volume of sediments available may not be high. Processes such as the ones recorded in closed lacustrine systems controlled by groundwater upwelling could occupy most of the geological time but may contribute volumetrically far less sediment to the sedimentary record, compared to more catastrophic events (e.g., sediment gravity flow and flash floods; Ager, 1986; Miall, 2016; Sadler, 1981). More recently, Kemp and Sadler (2014) demonstrated that the number and duration of intervals of nondeposition or erosion increases over time. In stratigraphy it is also now recognized that the duration of the gaps, the distribution of layer thicknesses and the sedimentation rate have fractal properties (Bailey & Smith, 2005; Plotnick, 1986; Sadler, 1999; Schlager, 2004; D. G. Smith et al., 2015). Furthermore, a recent Martian model proposed by Horvath and Andrews-Hanna (2017) predicts the presence of numerous small lakes around

Gale crater even if there are no sediments preserved within them or other geological evidence that supports past groundwater upwelling events.

Some of the craters studied in this work record a limited amount of deposits (i.e., not comparable with the layered mounds in shallower craters inside Arabia Terra and Meridiani Planum). The evidence supporting groundwater upwelling discussed by Andrews-Hanna et al. (2007, 2010) and Andrews-Hanna and Lewis (2011) are largely related to the layered sediments in the plains and within some craters in Arabia Terra. Different depositional rates depend on the different depositional processes involved even in the presence of a common control (in this case groundwater fluctuations).

The craters presented here show interior valleys that could potentially be attributed to sapping and also extremely flat floors that could potentially indicate the former presence of a groundwater-fed lake. Regardless, the lack of extensive sedimentary succession in deep craters, which would have experienced the first upwelling events compared to the shallower craters and intercrater plains (Andrews-Hanna & Lewis, 2011; Andrews-Hanna et al., 2007, 2010; Zabrusky et al., 2012), might appear to question the occurrence of groundwater upwelling. Zabrusky et al. (2012) hypothesized that erosional processes could have played a significant role in the lack of sedimentary deposits inside these deep basins, even if it would require erosional rates higher than expected (Golombek et al., 2006; Salese et al., 2016).

Again, the key question resides in understanding the nature of the depositional environments. The deepest basins do not necessarily share the same geological evolution (and consequently the same sedimentation rate) with the shallower basins in Arabia Terra and Meridiani Planum or the same erosional and depositional conditions.

The basins and the intercrater plains of Arabia Terra and Meridiani Planum appear to host mostly evaporitic deposition in playas (Grotzinger et al., 2005; Squyres et al., 2009) and possibly fluid upwelling in the same regions, such as spring mounds, as is suggested by the overall sulfate-bearing composition (Allen & Oehler, 2008; Pondrelli et al., 2015, 2011). Here the model used the groundwater upwelling scenario (Andrews-Hanna et al., 2010).

In the deepest basins, groundwater upwelling would have resulted in the formation of clastic-dominated fluviolacustrine depositional environments (with related subenvironments), while in the shallower basins/plains evaporitic deposition would have predominated. Clastic-dominated fluviolacustrine depositional environments entail the accumulation of most of the sediments in the proximal part of the basin (delta and shorelines), whereas the distal parts (i.e., central part of the lacustrine system/crater) can show very limited sediment accumulations. Moreover, as a consequence of the low sedimentation rate, diagenesis might have not occurred. The observed landforms and their relation to groundwater upwelling processes are also supported with mineralogical observations that suggest spectral evidence for Mg-rich clay minerals—possibly smectites and smectite/talc interlayered clays—as well as Mg carbonates (e.g., McLaughlin crater; Michalski et al., 2013). These minerals represent the typical manifestation of ancient groundwater processes on Mars, and they corroborate the hypothesis of lacustrine activity in these basins. This would imply a more complex geological relation between phyllosilicate and sulfate-bearing deposits than the mere sharp vertical transition that has been previously hypothesized (Bibring et al., 2006). The lateral transitions and interfingering found are also consistent with the detailed stratigraphies observed by the in situ analyses performed by rovers (Cino et al., 2017).

4.3. Groundwater or Precipitation Control?

In our work we found a sustained water level variation of at least 800 m between the investigated craters. We do not take into account the apex of sapping valleys because they could be affected by a certain degree of uncertainty due to recessive erosion of the valleys, especially if we take into account a composite discharge model in the development of the valleys. The range of sustained water level variation that we estimated from several geological observations is of the same order of magnitude estimated by the model of Horvath and Andrews-Hanna (2017) for Gale crater. There is a notable consistency between the stationary water level at approximately −4,000 m in the basins analyzed and previous works that suggests the presence of a northern Late Hesperian ocean shoreline between 3,940 and −4,100 m (Costard et al., 2017; Ivanov et al., 2017J. A. Rodriguez et al., 2016; Webb, 2004). Ivanov et al. (2017) also date the Deuteronilus shoreline to 3.6 Ga, which is close to the model ages of several of the craters studied in this work (see Table S1 for crater age estimation).

This supports putative post Noachian sedimentary deposits within the studied basins and the notion that there was a link between the ocean and a planet-wide groundwater system as well.

The outflow channels also form part of this emerging picture of a planet-wide groundwater table linked to the ocean. The outflow channels might have been fed by this groundwater system as suggested by previous authors for specific areas (Marra et al., 2015; J. A. P. Rodriguez, Kargel, et al., 2015). As proposed in previous work (Baker, 2001; Baker et al., 1991; Clifford & Parker, 2001; Fairen et al., 2003; Parker et al., 1993, 1989; Tanaka et al., 2005), groundwater outbursts at the end of the Hesperian may have generated catastrophic floods flowing through the outflow channels into the ocean in the northern lowlands.

Different climatic conditions can strongly influence the variation of the groundwater level as shown by Horvath and Andrews-Hanna (2017). The parameters that most affect the groundwater level are the aridity index and the annual precipitation. For a given aridity index, the lack or reduction of precipitation leads to a lower recharge of the aquifers and therefore a lowering of the groundwater level. A recent precipitation-based theory work by Seybold et al. (2018) analyzed branching geometry of valley networks both on Earth and Mars concluding that Martian valleys formed primarily by overland flow erosion and that groundwater seepage played a minor role. Nevertheless, valleys that fed the basins studied in our work are not branched and their morphology is consistent with a sapping-like and/or mixed origin.

Permeability also controls the aquifer: as it increases, subsurface flow becomes a prominent source to the lake, allowing a given lake to persist even in arid climates. Furthermore, different degrees of aqueous-related activity in the craters could be due to lateral and vertical variations in permeability because of different primary and/or postdepositional lithological characters. Horvath and Andrews-Hanna (2017) estimated a possible variation of the water surface within Gale crater of about 600 m depending on different climatic conditions. Nevertheless, the authors did not find any geological evidence of lakes inside the craters surrounding Gale, which could corroborate and confirm their results. Our studied basins can be an excellent case study to test in future works the Horvath and Andrews-Hanna (2017) model in the presence of integrated geological evidence.

5. Conclusions

The studied basins show evidence of water-related landforms below −4,000-m Mars datum. This suggests that the water-saturated zone and any long-term stationary water level remained below an elevation of −4,000 m. Nevertheless, the existence of such a deep aquifer does not exclude the presence of other aquifers at lower elevation, such as the one inferred for the Endeavour crater explored by MER Opportunity. Other aquifers could have existed in Martian history depending on either lateral or vertical stratigraphy. In the deepest basins, groundwater upwelling would have resulted in the formation of clastic-dominated fluvio-lacustrine depositional environments (with related subenvironments), as also demonstrated by the presence of Gilbert delta, while in the shallower basins/plains evaporitic deposition would have predominated.

These observations suggest that only the deepest basins, those with floors deeper than −4,000 m below the Mars datum, intercepted this deep water-saturated zone. Furthermore, they point toward the existence of a planet-wide groundwater table between −4,000 and −5,000 m during the past Martian history. This evidence fully or partially supports the models proposed by Andrews-Hanna and Lewis (2011); Michalski et al. (2013), which predicted regional to global groundwater upwelling and the existence of a water saturated zone around −4,000 m below Mars datum respectively. Basins with bases deeper than −4000 m below Mars datum intercepted the water-saturated zone were predicted by the model of Michalski et al. (2013) and exhibit evidence of groundwater fluctuations.

The analysis of these morphologies shows that the topographic elevation of the water surface fluctuated at least between −4,000 and −4,800 m (Table 1), but at a certain point in time it became sufficiently stable to allow the formation of deltas. The range of water level variations that we estimated from several geological observations is of the same order of magnitude as the one estimated by the model of Horvath and Andrews-Hanna (2017) for Gale crater. Fifteen of the 24 deep basins analyzed in our study show clear evidence of the existence of deltas or stepped deltas (Figure 1). Other morphological features also reinforce the idea of a stable water table, for example, the lowest part of the channels and the highest part of the terraces are notably at the same elevation as the deltas. Other morphologies that resulted from groundwater processes are

sapping valleys which, given the lack of surface drainage recharge and the absence of breached rims, represent the most compelling evidence that these basins were groundwater fed. The formation of sapping valleys at higher elevations than the groundwater basal level could have been possible due to the presence of the dike-confined water that can make the groundwater level shallower than the basal one. This concept is introduced for the first time in the Martian geological literature by the proposed conceptual model (Figure 2). In some craters we found stepped retrograding deltas indicating that over time the water level stabilized at different elevations and when the water level fell, the deltas were partially carved by channels and destroyed by erosion.

It is notable that the position of the water table varied within a range between −4,800 and −4,000 m in all 24 basins that exhibit water related landforms. This may suggest that the aquifer in all basins was interconnected; nevertheless, the evidence obtained from this work is not enough to affirm with certainty the interbasins connection. Our observations show that the extent of this aquifer is very significant and it leads us to support the thesis that it could have been planet wide.

Supporting information: It is linked to the online version of the paper.

Acknowledgments
Francesco Salese was supported by Marie Curie Individual Postdoctoral Fellowship (WET_MARS, Grant Agreement 795192). We would like to thank Monica Bufill for her time spent on reviewing our manuscript and her comments helping us improving the article and two anonymous reviewers. The data (HRSC, CTX, HiRISE, and MOLA) that support the findings of this study were obtained freely from the Planetary Data System (PDS) and are publicly available online at https://pds.nasa.gov/index.shtml. The authors wish to thank MRO and HRSC team for these data. Satellite imagery and the Extended Data were generated with ISIS 3 (Integrated Software for Imagers and Spectrometers) available online at https://isis.astrogeology.usgs.gov. All these data were integrated into ArcGIS 10.6 project. Correspondence and requests for materials should be addressed to F. S (f.salese@uu.nl).

References

Ager, D. V. (1981). *The nature of the stratigraphical record*, (2nd ed.). New York: John Wiley.
Ager, D. V. (1986). A reinterpretation of the basal "Littoral Lias" of the Vale of Glamorgan. *Proceedings of the Geologists' Association*, *97*(1), 29–35. https://doi.org/10.1016/S0016-7878(86)80003-7
Allen, C. C., & Oehler, D. Z. (2008). A case for ancient springs in Arabia Terra, Mars. *Astrobiology*, *8*(6), 1093–1112. https://doi.org/10.1089/ast.2008.0239
Amidon, W. H., & Clark, A. C. (2015). Interaction of outburst floods with basaltic aquifers on the Snake River Plain: Implications for Martian canyons. *Geological Society of America Bulletin*, *127*(5–6), 688–701. https://doi.org/10.1130/B31141.1
Andrews-Hanna, J. C., & Lewis, K. W. (2011). Early Mars hydrology: 2. Hydrological evolution in the Noachian and Hesperian epochs. *Journal of Geophysical Research*, *116*, E02007. https://doi.org/10.1029/2010je003709
Andrews-Hanna, J. C., Phillips, R. J., & Zuber, M. T. (2007). Meridiani Planum and the global hydrology of Mars. *Nature*, *446*(7132), 163–166. https://doi.org/10.1038/nature05594
Andrews-Hanna, J. C., Zuber, M. T., Arvidson, R. E., & Wiseman, S. M. (2010). Early Mars hydrology: Meridiani playa deposits and the sedimentary record of Arabia Terra. *Journal of Geophysical Research*, *115*, E06002. https://doi.org/10.1029/2009je003485
Bailey, R. J., & Smith, D. G. (2005). Quantitative evidence for the fractal nature of the stratigraphie record: Results and implications. *Proceedings of the Geologists' Association*, *116*(2), 129–138. https://doi.org/10.1016/S0016-7878(05)80004-5
Baker, V. R. (2001). Water and the Martian landscape. *Nature*, *412*(6843), 228–236. https://doi.org/10.1038/35084172
Baker, V. R., Strom, R. G., Gulick, V. C., Kargel, J. S., Komatsu, G., & Kale, V. S. (1991). Ancient oceans, ice sheets and the hydrological cycle on Mars. *Nature*, *352*(6336), 589–594. https://doi.org/10.1038/352589a0
Banerdt, W. B., Phillips, R. J., Sleep, N. H., & Saunders, R. S. (1982). Thick shell tectonics on one-plate planets: Applications to Mars. *Journal of Geophysical Research*, *87*(B12), 9723–9733. https://doi.org/10.1029/JB087iB12p09723
Bibring, J. P., Langevin, Y., Mustard, J. F., Poulet, F., Arvidson, R., Gendrin, A., et al. (2006). Global mineralogical and aqueous mars history derived from OMEGA/Mars Express data. *Science*, *312*(5772), 400–404. https://doi.org/10.1126/science.1122659
Breuer, D., & Spohn, T. (2003). Early plate tectonics versus single-plate tectonics on Mars: Evidence from magnetic field history and crust evolution. *Journal of Geophysical Research*, *108*(E7), 5072. https://doi.org/10.1029/2002JE001999
Cabrol, N. A., & Grin, E. A. (1999). Distribution, classification, and ages of Martian impact crater lakes. *Icarus*, *142*(1), 160–172. https://doi.org/10.1006/icar.1999.6191
Carr, M. H., & Head, J. W. (2003). Oceans on Mars: An assessment of the observational evidence and possible fate. *Journal of Geophysical Research*, *108*(E5), 5042. https://doi.org/10.1029/2002je001963
Carr, M. H., & Head, J. W. (2010). Geologic history of Mars. *Earth and Planetary Science Letters*, *294*(3–4), 185–203. https://doi.org/10.1016/j.epsl.2009.06.042
Carrozzo, F. G., Di Achille, G., Salese, F., Altieri, F., & Bellucci, G. (2017). Geology and mineralogy of the Auki Crater, Tyrrhena Terra, Mars: A possible post impact-induced hydrothermal system. *Icarus*, *281*, 228–239. https://doi.org/10.1016/j.icarus.2016.09.001
Chan, M. A., Beitler, B., Parry, W. T., Ormo, J., & Komatsu, G. (2004). A possible terrestrial analogue for haematite concretions on Mars. *Nature*, *429*(6993), 731–734. https://doi.org/10.1038/nature02600
Cino, C. D., Dehouck, E., & McLennan, S. M. (2017). Geochemical constraints on the presence of clay minerals in the burns formation, Meridiani Planum, Mars. *Icarus*, *281*, 137–150. https://doi.org/10.1016/j.icarus.2016.08.029
Clifford, S. M., & Parker, T. J. (2001). The evolution of the Martian hydrosphere: Implications for the fate of a primordial ocean and the current state of the northern plains. *Icarus*, *154*(1), 40–79. https://doi.org/10.1006/icar.2001.6671
Costard, F., Sejourne, A., Kelfoun, K., Clifford, S., Lavigne, F., Di Pietro, I., & Bouley, S. (2017). Modeling tsunami propagation and the emplacement of thumbprint terrain in an early Mars Ocean. *Journal of Geophysical Research: Planets*, *122*, 633–649. https://doi.org/10.1002/2016je005230
De Hon, R. A. (1992). Martian lake basins and lacustrine plains. *Earth, Moon, and Planets*, *56*(2), 95–122. https://doi.org/10.1007/BF00056352
Dott, R. H. (1983). 1982 Sepm Presidential-Address—Episodic sedimentation—How normal is average—How rare is rare—Does it matter. *Journal of Sedimentary Petrology*, *53*(1), 5–23. https://doi.org/10.1306/212f8148-2b24-11d7-8648000102c1865d
Fairen, A. G., Dohm, J. M., Baker, V. R., de Pablo, M. A., Ruiz, J., Ferris, J. C., & Anderson, R. C. (2003). Episodic flood inundations of the northern plains of Mars. *Icarus*, *165*(1), 53–67. https://doi.org/10.1016/S0019-1035(03)00144-1
Fassett, C. I., & Head, J. W. (2008). Valley network-fed, open-basin lakes on Mars: Distribution and implications for Noachian surface and subsurface hydrology. *Icarus*, *198*(1), 37–56. https://doi.org/10.1016/j.icarus.2008.06.016

Gilbert, G. K. (1885). *The topographic features of lake shores*. WA: US Government Printing Office.
Goldspiel, J. M., & Squyres, S. W. (2000). Groundwater sapping and valley formation on Mars. *Icarus*, *148*(1), 176–192. https://doi.org/10.1006/icar.2000.6465
Golombek, M. P., Grant, J. A., Crumpler, L. S., Greeley, R., Arvidson, R. E., Bell, J. F., et al. (2006). Erosion rates at the Mars exploration rover landing sites and long-term climate change on Mars. *Journal of Geophysical Research*, *111*, E12S10. https://doi.org/10.1029/2006JE002754
Goudge, T. A., Aureli, K. L., Head, J. W., Fassett, C. I., & Mustard, J. F. (2015). Classification and analysis of candidate impact crater-hosted closed-basin lakes on Mars. *Icarus*, *260*, 346–367. https://doi.org/10.1016/j.icarus.2015.07.026
Grotzinger, J. P., Arvidson, R. E., Bell, J. F. III, Calvin, W., Clark, B. C., Fike, D. A., et al. (2005). Stratigraphy and sedimentology of a dry to wet eolian depositional system, Burns formation, Meridiani Planum, Mars. *Earth and Planetary Science Letters*, *240*(1), 11–72. https://doi.org/10.1016/j.epsl.2005.09.039
Hamilton, C. W., Mouginis-Mark, P. J., Sori, M. M., Scheidt, S. P., & Bramson, A. M. (2018). Episodes of aqueous flooding and effusive volcanism associated with Hrad Vallis, Mars. *Journal of Geophysical Research: Planets*, *123*(6), 1484–1510. https://doi.org/10.1029/2018je005543
Harrison, K. P., & Grimm, R. E. (2005). Groundwater-controlled valley networks and the decline of surface runoff on early Mars. *Journal of Geophysical Research*, *110*, E12S16. https://doi.org/10.1029/2005JE002455
Hauber, E., Reiss, D., Ulrich, M., Preusker, F., Trauthan, F., Zanetti, M., et al. (2011). Landscape evolution in Martian mid-latitude regions: Insights from analogous periglacial landforms in Svalbard. *Geological Society, London, Special Publications*, *356*(1), 111–131. https://doi.org/10.1144/SP356.7
Head, J. W. 3rd, Hiesinger, H., Ivanov, M. A., Kreslavsky, M. A., Pratt, S., & Thomson, B. J. (1999). Possible ancient oceans on Mars: Evidence from Mars Orbiter Laser Altimeter data. *Science*, *286*(5447), 2134–2137. https://doi.org/10.1126/science.286.5447.2134
Horvath, D. G., & Andrews-Hanna, J. C. (2017). Reconstructing the past climate at Gale crater, Mars, from hydrological modeling of late-stage lakes. *Geophysical Research Letters*, *44*, 8196–8204. https://doi.org/10.1002/2017GL074654
Howard, A. D. (1986). Groundwater sapping on Mars and Earth, paper presented at Proc., and Field Guide, NASA Groundwater Sapping Conf., AD Howard, RC Kochel, and HE Holt, Eds., National Aeronautics and Space Administration, Flagstaff, Ariz., pp. vi–xiv.
Howard, A. D., & Mclane, C. F. (1988). Erosion of cohesionless sediment by groundwater seepage. *Water Resources Research*, *24*(10), 1659–1674. https://doi.org/10.1029/WR024i010p01659
Ivanov, M. A., Erkeling, G., Hiesinger, H., Bernhardt, H., & Reiss, D. (2017). Topography of the Deuteronilus contact on Mars: Evidence for an ancient water/mud ocean and long-wavelength topographic readjustments. *Planetary and Space Science*, *144*, 49–70. https://doi.org/10.1016/j.pss.2017.05.012
Izuka, S. K., Engott, J. A., Rotzoll, K., Bassiouni, M., Johnson, A. G., Miller, L. D., & Mair, A. (2018). Volcanic aquifers of Hawai'i—Hydrogeology, water budgets, and conceptual models, *Report Rep*. 2015–*5164*, 172 pp, Reston, VA.
Jaumann, R., Neukum, G., Behnke, T., Duxbury, T. C., Eichentopf, K., Flohrer, J., et al. (2007). The high-resolution stereo camera (HRSC) experiment on Mars Express: Instrument aspects and experiment conduct from interplanetary cruise through the nominal mission. *Planetary and Space Science*, *55*(7–8), 928–952. https://doi.org/10.1016/j.pss.2006.12.003
Kemp, D. B., & Sadler, P. M. (2014). Climatic and eustatic signals in a global compilation of shallow marine carbonate accumulation rates. *Sedimentology*, *61*(5), 1286–1297. https://doi.org/10.1111/sed.12112
Kochel, R. C., & Piper, J. F. (1986). Morphology of large valleys on Hawaii—Evidence for groundwater sapping and comparisons with Martian valleys. *Journal of Geophysical Research*, *91*(B13), E175–E192. https://doi.org/10.1029/JB091iB13p0E175
Kreslavsky, M. A., & Head, J. W. (2002). Fate of outflow channel effluents in the northern lowlands of Mars: The Vastitas Borealis Formation as a sublimation residue from frozen ponded bodies of water. *Journal of Geophysical Research*, *107*(E12), 5121. https://doi.org/10.1029/2001je001831
Laity, J. E., & Malin, M. C. (1985). Sapping Processes and the Development of Theater-Headed Valley Networks on the Colorado Plateau. *Geological Society of America Bulletin*, *96*(2), 203–217. https://doi.org/10.1130/0016-7606(1985)96<203:Spatdo>2.0.Co;2
Lamb, M. P., Dietrich, W. E., Aciego, S. M., Depaolo, D. J., & Manga, M. (2008). Formation of Box Canyon, Idaho, by megaflood: Implications for seepage erosion on Earth and Mars. *Science*, *320*(5879), 1067–1070. https://doi.org/10.1126/science.1156630
Lamb, M. P., Grotzinger, J. P., Southard, J. B., & Tosca, N. J. (2012). Were aqueous ripples on Mars formed by flowing brines?
Lamb, M. P., Howard, A. D., Johnson, J., Whipple, K. X., Dietrich, W. E., & Perron, J. T. (2006). Can springs cut canyons into rock? *Journal of Geophysical Research*, *111*, E07002. https://doi.org/10.1029/2005JE002663
Lapotre, M. G. A., & Lamb, M. P. (2018). Substrate controls on valley formation by groundwater on Earth and Mars. *Geology*, *46*(6), 531–534. https://doi.org/10.1130/G40007.1
Loizeau, D., Werner, S. C., Mangold, N., Bibring, J. P., & Vago, J. L. (2012). Chronology of deposition and alteration in the Mawrth Vallis region, Mars. *Planetary and Space Science*, *72*(1), 31–43. https://doi.org/10.1016/j.pss.2012.06.023
Macdonald, G. A., Abbott, A. T., & Peterson, F. L. (1983). *Volcanoes in the sea: The geology of Hawaii*. Honolulu, HI: University Of Hawaii Press.
Malin, M. C., Bell, J. F. III, Cantor, B. A., Caplinger, M. A., Calvin, W. M., Clancy, R. T., et al. (2007). Context Camera Investigation on board the Mars Reconnaissance Orbiter. *Journal of Geophysical Research*, *112*, E05s04. https://doi.org/10.1029/2006je002808
Malin, M. C., & Carr, M. H. (1999). Groundwater formation of Martian valleys. *Nature*, *397*(6720), 589–591. https://doi.org/10.1038/17551
Malin, M. C., & Edgett, K. S. (1999). Oceans or seas in the Martian northern lowlands: High resolution imaging tests of proposed coastlines. *Geophysical Research Letters*, *26*(19), 3049–3052. https://doi.org/10.1029/1999gl002342
Mangold, N., Ansan, V., Masson, P., Quantin, C., & Neukum, G. (2008). Geomorphic study of fluvial landforms on the northern Valles Marineris plateau, Mars. *Journal of Geophysical Research*, *113*, E08009. https://doi.org/10.1029/2007je002985
Marra, W. A., Braat, L., Baar, A. W., & Kleinhans, M. G. (2014). Valley formation by groundwater seepage, pressurized groundwater outbursts and crater-lake overflow in flume experiments with implications for Mars. *Icarus*, *232*, 97–117. https://doi.org/10.1016/j.icarus.2013.12.026
Marra, W. A., Hauber, E., de Jong, S. M., & Kleinhans, M. G. (2015). Pressurized groundwater systems in Lunae and Ophir Plana (Mars): Insights from small-scale morphology and experiments. *GeoResJ*, *8*, 1–13. https://doi.org/10.1016/j.grj.2015.08.001
Masson, D. G., Harbitz, C. B., Wynn, R. B., Pedersen, G., & Lovholt, F. (2006). Submarine landslides: Processes, triggers and hazard prediction. *Philosophical Transactions. Series A, Mathematical, Physical, and Engineering Sciences*, *364*(1845), 2009–2039. https://doi.org/10.1098/rsta.2006.1810
McEwen, A. S., Eliason, E. M., Bergstrom, J. W., Bridges, N. T., Hansen, C. J., Delamere, W. A., et al. (2007). Mars Reconnaissance Orbiter's High Resolution Imaging Science Experiment (HiRISE). *Journal of Geophysical Research*, *112*, E05s02. https://doi.org/10.1029/2005je002605

Miall, A. D. (2016). Stratigraphy: The modern synthesis. In *Stratigraphy: A modern synthesis* (pp. 311–370). Berlin, Germany: Springer.
Michalski, J. R., Cuadros, J., Niles, P. B., Parnell, J., Rogers, A. D., & Wright, S. P. (2013). Groundwater activity on Mars and implications for a deep biosphere. *Nature Geoscience*, *6*(2), 133–138. https://doi.org/10.1038/Ngeo1706
Michalski, J. R., Rogers, A. D., Wright, S. P., Niles, P., & Cuadros, J. (2012). Sporadic groundwater upwelling in deep Martian craters: Evidence for lacustrine clays and carbonates.
Michaux, C. M., & Newburn, R. L. Jr (1972). Mars scientific model JPL doc. 606-1Jet Propul, Lab., *Pasadena, Calif*.
Murchie, S., Arvidson, R., Bedini, P., Beisser, K., Bibring, J. P., Bishop, J., et al. (2007). Compact reconnaissance Imaging Spectrometer for Mars (CRISM) on Mars Reconnaissance Orbiter (MRO). *Journal of Geophysical Research*, *112*, E05s03. https://doi.org/10.1029/2006je002682
Neukum, G., & Jaumann, R. (2004). HRSC: The high resolution stereo camera of Mars Express, paper presented at Mars Express: The Scientific Payload.
Ori, G. G., Marinangeli, L., & Baliva, A. (2000). Terraces and Gilbert-type deltas in crater lakes in Ismenius Lacus and Memnonia (Mars). *Journal of Geophysical Research*, *105*(E7), 17,629–17,641. https://doi.org/10.1029/1999JE001219
Ori, G. G., & Mosangini, C. (1998). Complex depositional systems in Hydraotes Chaos, Mars: An example of sedimentary process interactions in the Martian hydrological cycle. *Journal of Geophysical Research*, *103*(E10), 22,713–22,723. https://doi.org/10.1029/98JE01969
Pain, C. F., & Ollier, C. D. (1995). Regolith stratigraphy: Principles and problems. *AGSO Journal of Australian Geology and Geophysics*, *16*(3), 197–202.
Palucis, M. C., Dietrich, W. E., Williams, R. M. E., Hayes, A. G., Parker, T., Sumner, D. Y., et al. (2016). Sequence and relative timing of large lakes in Gale crater (Mars) after the formation of Mount Sharp. *Journal of Geophysical Research: Planets*, *121*, 472–496. https://doi.org/10.1002/2015je004905
Parker, T. J., Gorsline, D. S., Saunders, R. S., Pieri, D. C., & Schneeberger, D. M. (1993). Coastal geomorphology of the Martian Northern Plains. *Journal of Geophysical Research*, *98*(E6), 11,061–11,078. https://doi.org/10.1029/93je00618
Parker, T. J., Saunders, R. S., & Schneeberger, D. M. (1989). Transitional morphology in West Deuteronilus Mensae, Mars - implications for modification of the lowland upland boundary. *Icarus*, *82*(1), 111–145. https://doi.org/10.1016/0019-1035(89)90027-4
Pelletier, J. D., & Baker, V. R. (2011). The role of weathering in the formation of bedrock valleys on Earth and Mars: A numerical modeling investigation. *Journal of Geophysical Research*, *116*, E11007. https://doi.org/10.1029/2011je003821
Peterson, F. L. (1972). Water development on tropic Volcanic Islands—Type example: Hawaii a. *Groundwater*, *10*(5), 18–23. https://doi.org/10.1111/j.1745-6584.1972.tb03586.x
Platz, T., Michael, G., Tanaka, K. L., Skinner, J. A., & Fortezzo, C. M. (2013). Crater-based dating of geological units on Mars: Methods and application for the new global geological map. *Icarus*, *225*(1), 806–827. https://doi.org/10.1016/j.icarus.2013.04.021
Plotnick, R. E. (1986). A fractal model for the distribution of stratigraphic hiatuses. *Journal of Geology*, *94*(6), 885–890. https://doi.org/10.1086/629094
Pondrelli, M., Rossi, A. P., Le Deit, L., Fueten, F., van Gasselt, S., Glamoclija, M., et al. (2015). Equatorial layered deposits in Arabia Terra, Mars: Facies and process variability. *Geological Society of America Bulletin*, *127*(7–8), B31225.1–B31225.1089. https://doi.org/10.1130/B31225.1
Pondrelli, M., Rossi, A. P., Ori, G. G., van Gasselt, S., Praeg, D., & Ceramicola, S. (2011). Mud volcanoes in the geologic record of Mars: The case of Firsoff crater. *Earth and Planetary Science Letters*, *304*(3–4), 511–519. https://doi.org/10.1016/j.epsl.2011.02.027
Postma, G. (1990). Depositional architecture and facies of river and fan deltas: A synthesis, in *Coarse-grained deltas*, *Special Publication* (Vol. 10, pp. 13-27). Gent, Belgium: International Association of Sedimentologists.
Prior, D. B. (1988). Submarine morphology and processes of fjord fan deltas and related high-gradient systems: Modern examples from British Columbia, Fan delta: ssedimen-tology and tectonic settings, 125-143.
Robbins, S. J., & Hynek, B. M. (2012). A new global database of Mars impact craters≥ 1 km: 2. Global crater properties and regional variations of the simple-to-complex transition diameter. *Journal of Geophysical Research*, *117*, E06001. https://doi.org/10.1029/2011JE003967
Rodriguez, J. A., Fairén, A. G., Tanaka, K. L., Zarroca, M., Linares, R., Platz, T., et al. (2016). Tsunami waves extensively resurfaced the shorelines of an early Martian Ocean. *Scientific Reports*, *6*(1), 25106. https://doi.org/10.1038/srep25106
Rodriguez, J. A. P., Kargel, J. S., Baker, V. R., Gulick, V. C., Berman, D. C., Fairén, A. G., et al. (2015). Martian outflow channels: How did their source aquifers form, and why did they drain so rapidly? *Scientific Reports*, *5*(1), 13404. https://doi.org/10.1038/srep13404
Rodriguez, J. A. P., Zarroca, M., Linares, R., Gulick, V., Weitz, C. M., Yan, J., et al. (2015). Groundwater flow induced collapse and flooding in Noctis Labyrinthus, Mars. *Planetary and Space Science*, *124*, 1–14. https://doi.org/10.1016/j.pss.2015.12.009.
Ruj, T., Komatsu, G., Dohm, J. M., Miyamoto, H., & Salese, F. (2017). Generic identification and classification of morphostructures in the Noachis-Sabaea region, southern highlands of Mars. *Journal of Maps*, *13*(2), 755–766. https://doi.org/10.1080/17445647.2017.1379913
Sadler, P. M. (1981). Sediment accumulation rates and the completeness of stratigraphic sections. *Journal of Geology*, *89*(5), 569–584. https://doi.org/10.1086/628623
Sadler, P. M. (1999). The influence of hiatuses on sediment accumulation rates, Paper Presented at GeoResearch Forum.
Salese, F., Ansan, V., Mangold, N., Carter, J., Ody, A., Poulet, F., & Ori, G. G. (2016). A sedimentary origin for intercrater plains north of the Hellas basin: Implications for climate conditions and erosion rates on early Mars. *Journal of Geophysical Research: Planets*, *121*, 2239–2267. https://doi.org/10.1002/2016je005039
Schlager, W. (2004). Fractal nature of stratigraphic sequences. *Geology*, *32*(3), 185–188. https://doi.org/10.1130/G202531.1.
Schumm, S. A., Boyd, K. F., Wolff, C. G., & Spitz, W. J. (1995). A ground-water sapping landscape in the Florida Panhandle. *Geomorphology*, *12*(4), 281–297. https://doi.org/10.1016/0169-555X(95)00011-S
Scott, D. H., Dohm, J. M., & Rice Jr, J. W. (1995). Map of Mars showing channels and possible paleolake basins*Rep*.
Scott, D. H., Rice, J. W., & Dohm, J. M. (1991). Martian Paleolakes and waterways—Exobiological implications. *Origins of Life and Evolution of the Biosphere*, *21*(3), 189–198. https://doi.org/10.1007/Bf01809447
Seybold, H. J., Kite, E., & Kirchner, J. W. (2018). Branching geometry of valley networks on Mars and earth and its implications for early Martian climate. *Science Advances*, *4*(6), eaar6692. https://doi.org/10.1126/sciadv.aar6692
Sharp, R. P., & Malin, M. C. (1975). Channels on Mars. *Geological Society of America Bulletin*, *86*(5), 593–609. https://doi.org/10.1130/0016-7606(1975)86<593:Com>2.0.Co;2
Siebach, K. L., Grotzinger, J. P., Kah, L. C., Stack, K. M., Malin, M., Leveille, R., & Sumner, D. Y. (2014). Subaqueous shrinkage cracks in the Sheepbed mudstone: Implications for early fluid diagenesis, Gale crater, Mars. *Journal of Geophysical Research: Planets*, *119*, 1597–1613. https://doi.org/10.1002/2014je004623
Slipher, E. C. (1962). The photographic story of Mars, *Cambridge, Mass.,* Sky Pub. Corp., 1962.

Smith, D. E., Zuber, M. T., Solomon, S. C., Phillips, R. J., Head, J. W., Garvin, J. B., et al. (1999). The global topography of Mars and implications for surface evolution. *Science*, *284*(5419), 1495–1503. https://doi.org/10.1126/science.284.5419.1495

Smith, D. G., Bailey, R. J., Burgess, P. M., & Fraser, A. J. (2015). Strata and time: Probing the gaps in our understanding. *Geological Society, London, Special Publications*, *404*, 1–10. https://doi.org/10.1144/SP404.16

Squyres, S. W., Grotzinger, J. P., Arvidson, R. E., Bell, J. F. III, Calvin, W., Christensen, P. R., et al. (2004). In situ evidence for an ancient aqueous environment at Meridiani Planum, Mars. *Science*, *306*(5702), 1709–1714. https://doi.org/10.1126/science.1104559

Squyres, S. W., Knoll, A. H., Arvidson, R. E., Ashley, J. W., Bell, J. F., Calvin, W. M., et al. (2009). Exploration of Victoria crater by the Mars rover Opportunity. *Science*, *324*(5930), 1058–1061. https://doi.org/10.1126/science.1170355

Stack, K. M., Grotzinger, J. P., Kah, L. C., Schmidt, M. E., Mangold, N., Edgett, K. S., et al. (2014). Diagenetic origin of nodules in the Sheepbed member, Yellowknife Bay formation, Gale crater, Mars. *Journal of Geophysical Research: Planets*, *119*, 1637–1664. https://doi.org/10.1002/2014je004617

Stearns, H. T. (1966). *Geology of the State of Hawaii* (p. 266). Palo Alto, California: Pacific Books.

Tanaka, K. L., Robbins, S. J., Fortezzo, C. M., Skinner, J. A., & Hare, T. M. (2014). The digital global geologic map of Mars: Chronostratigraphic ages, topographic and crater morphologic characteristics, and updated resurfacing history. *Planetary and Space Science*, *95*, 11–24. https://doi.org/10.1016/j.pss.2013.03.006

Tanaka, K. L., Skinner, J. A., & Hare, T. M. (2005). Geologic map of the northern plains of Mars.

Tosca, N. J., Ahmed, I. A. M., Tutolo, B. M., Ashpitel, A., & Hurowitz, J. A. (2018). Magnetite authigenesis and the warming of early Mars. *Nature Geoscience*, *11*(9), 635–639. https://doi.org/10.1038/s41561-018-0203-8

Treiman, A. H. (2008). Ancient groundwater flow in the Valles Marineris on Mars inferred from fault trace ridges. *Nature Geoscience*, *1*(3), 181–183. https://doi.org/10.1038/ngeo131

Weaver, P. P. E., Wynn, R. B., Kenyon, N. H., & Evans, J. (2000). Continental margin sedimentation, with special reference to the north-east Atlantic margin. *Sedimentology*, *47*(s1), 239–256. https://doi.org/10.1046/j.1365-3091.2000.0470s1239.x

Webb, V. E. (2004). Putative shorelines in northern Arabia Terra, Mars. *Journal of Geophysical Research*, *109*(E9), 9010. https://doi.org/10.1029/2003je002205

Wray, J. J., Milliken, R. E., Dundas, C. M., Swayze, G. A., Andrews-Hanna, J. C., Baldridge, A. M., et al. (2011). Columbus crater and other possible groundwater-fed paleolakes of Terra Sirenum, Mars. *Journal of Geophysical Research*, *116*, E01001. https://doi.org/10.1029/2010JE003694

Zabrusky, K., Andrews-Hanna, J. C., & Wiseman, S. M. (2012). Reconstructing the distribution and depositional history of the sedimentary deposits of Arabia Terra, Mars. *Icarus*, *220*(2), 311–330. https://doi.org/10.1016/j.icarus.2012.05.007